Nanoscale

Accepted Manuscript

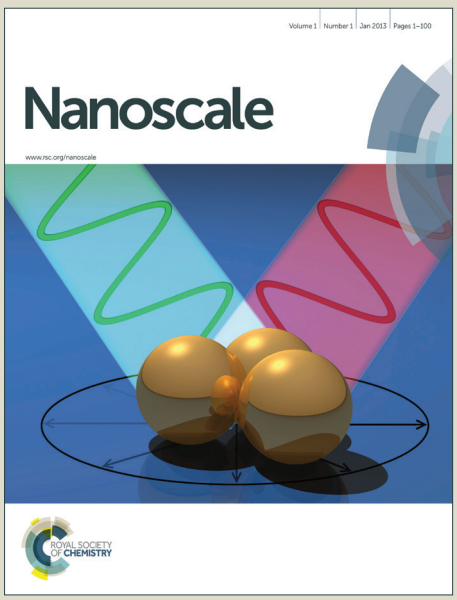

ROYAL SOCIETY OF CHEMISTRY

www.rsc.org/nanoscale

ARTICLE TYPE www. rsc.org/xxxxxx | XXXXXXXX

The use of atomic layer deposition in advanced nanopatterning

A.J.M. Mackus,[a] A.A. Bol,*[a] and W.M.M. Kessels[a]

Received Xth XXXXXXXXXX 20XX, Accepted Xth XXXXXXXXX 20XX
First published on the web Xth XXXXXXXXXX 200X
DOI: 10.1039/b000000x

Atomic layer deposition (ALD) is a method that allows for the deposition of thin films with atomic level control of the thickness and an excellent conformality on 3-dimensional surfaces. In recent years, ALD has been implemented in many applications in microelectronics, for which often a patterned film instead of a full area coverage is required. This article reviews several approaches for the patterning of ALD-grown films. In addition to conventional methods relying on etching, there has been much interest in nanopatterning by area-selective ALD. Area-selective approaches can eliminate compatibility issues associated with the use of etchants, lift-off chemicals, or resist films. Moreover, the use of ALD as an enabling technology in advanced nanopatterning methods such as spacer defined double patterning or block copolymer lithography is discussed, as well as the application of selective ALD in self-aligned fabrication schemes.

I. Introduction

Atomic layer deposition (ALD) is a vapor phase thin film deposition technique that enables the deposition of films with a high material quality, good uniformity, high conformality, and accurate thickness control.[1,2] ALD relies on the alternate pulsing of precursor and reactant gases, separated by purge steps, resulting in self-limiting surface reactions. Due to the cyclic nature of the process, the material is deposited layer-by-layer, which gives an unparalleled control of the film thickness on the atomic level. For most applications in microelectronics however, it is also required to control the lateral dimensions of the film by patterning. Patterned films are for example ubiquitous in transistor and interconnect technology, in which the basic building blocks typically consist of a stack of several patterned films of different materials. Since ALD has no intrinsic ability to control the lateral dimensions of the growth, patterning techniques need to be used to structure a blanket deposited film, or to limit the ALD growth to specific surface areas. The conventional approach for film structuring consists of the patterning of a resist layer by photolithography, followed by the transfer of the pattern by etching.

ALD offers opportunities for nanopatterning, for example, when working with the sensitive materials that are considered for future nanoelectronics such as organic layers, graphene,

[a] *Department of Applied Physics, Eindhoven University of Technology, P.O. Box 513, 5600 MB Eindhoven, the Netherlands. Tel: +31 40-247 5851; E-mail: a.a.bol@tue.nl*

Adrie Mackus (1985) earned his M.Sc. and Ph.D. degrees (both cum laude) in Applied Physics at Eindhoven University of Technology in 2009 and 2013, respectively. His doctoral thesis work focused on the development of novel nanopatterning approaches based on ALD, as well as on the study of metal ALD. Adrie currently works as a postdoc at Stanford University, where he investigates the reaction mechanisms of ALD processes with applications in solar cells.

Ageeth Bol is an assistant professor of applied physics at Eindhoven University of Technology, the Netherlands. She received her MSc and PhD in chemistry from Utrecht University, the Netherlands. After obtaining her PhD degree in 2001 she worked for Philips Electronics and at the IBM TJ Watson Research Center. In 2011 she joined the faculty of Eindhoven University of Technology. Her current research interests include the fabrication, modification and integration of 1-D and 2-D nanomaterials for nanodevice applications.

carbon nanotubes, or nanowires. Photolithography involves many processing steps, such as resist spinning, light exposure, resist development, and etching, and some of these steps may lead to compatibility issues with sensitive materials. In order to avoid etching, a lift-off approach can be employed in which the resist film is patterned prior to the film deposition. This requires the deposition of films at relatively low substrate temperatures to prevent damage to the resist layer, and this can be achieved by ALD.[3]

Since ALD depends critically on surface chemistry, it is also possible to chemically modify a surface to enable area-selective ALD.[4,5] Local modification of the surface properties opens up new approaches in which there is also lateral control of ALD film growth in addition to the thickness control of ALD. So far, most studies about area-selective ALD deal with the deactivation of areas of the surface by certain molecules, allowing for selective ALD on those areas that are not deactivated.[4,6] Recently, also a few methods have been introduced relying on local activation of the ALD growth.[7,8]

Moreover, ALD starts to play an important role in several advanced nanopatterning schemes. It is for example used to reduce the number of processing steps in lithographic process flows, or to modify the properties of resist films. These methods can be described as *ALD-enabled nanopatterning*. An important example is the application of ALD in spacer defined double patterning (SDDP), i.e. one of the resolution enhancement technologies that are currently under development now that the semiconductor industry is facing challenges with the implementation of EUV lithography.[9] ALD allows for the elimination of several processing steps because it is able to deposit ultrathin conformal layers at low substrate temperatures.[10,11]

Erwin Kessels is a full professor at the Eindhoven University of Technology TU/e where he is also the scientific director of the NanoLab@TU/e clean room facilities. Erwin received his M.Sc. and Ph.D. degree (cum laude) in Applied Physics from the TU/e in 1996 and 2000, respectively. His research interests cover the field of synthesis of ultrathin films and nanostructures using methods such as (plasma-enhanced) chemical vapor deposition (CVD) and atomic layer deposition (ALD) for a wide variety of applications, mostly within nanoelectronics and photovoltaics. A main focus lies on nanomanufacturing aiming at materials and dimensions control through atomic level understanding.

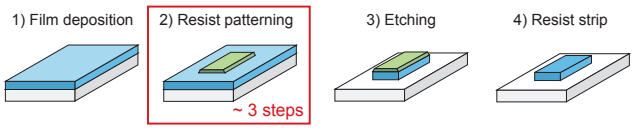

Fig. 1 Process flow of conventional patterning based on etching. The patterning of the resist layer typically involves three additional processing steps as illustrated in Fig. 2.

In this article, the use of ALD in advanced nanopatterning is reviewed. First, conventional patterning based on etching is presented as background information. Section III. deals with ALD-enabled nanopatterning, and describes the use of ALD in SDDP, as well as the modification of resist properties by ALD. In Sec. IV., the different methods for patterning of ALD-grown films are described: (*i*) patterning based on lithography and lift-off; (*ii*) area-selective ALD by area-deactivation; and (*iii*) area-selective ALD by area-activation. The benefits and drawbacks of these approaches are discussed. Sec. V. describes recent developments in the use of selective ALD in self-aligned fabrication schemes. The work on area-selective ALD has inspired new approaches for the synthesis of complex nanoscale structures. In Sec. VI., it is illustrated how knowledge obtained in studies on area-selective ALD has been exploited for the deposition of nanoparticles, nanotubes, and nanowires.

II. Conventional patterning

In this section, methods used in conventional patterning approaches are briefly described, which serves as background information for the following sections. The application of ALD in conventional nanopatterning is discussed at the end of the section.

Conventional patterning relies on the patterning of a resist film, followed by etching. Figure 1 schematically illustrates the typical process flow of a basic lithographic process. First, the material that needs to be structured is blanket-deposited on the substrate. Next, a resist layer is patterned on the film, by using for example photolithography, e-beam lithography (EBL), soft lithography or imprint lithography, as discussed in more detail below. This pattern subsequently needs to be transferred to the underlying film via an etching process. In wet etching, the sample is immersed in a chemical solution, which attacks the regions of the film that are not covered with the resist layer. In general, wet etching is isotropic, and cannot be used to fabricate fine features. Dry etching by plasma expo-

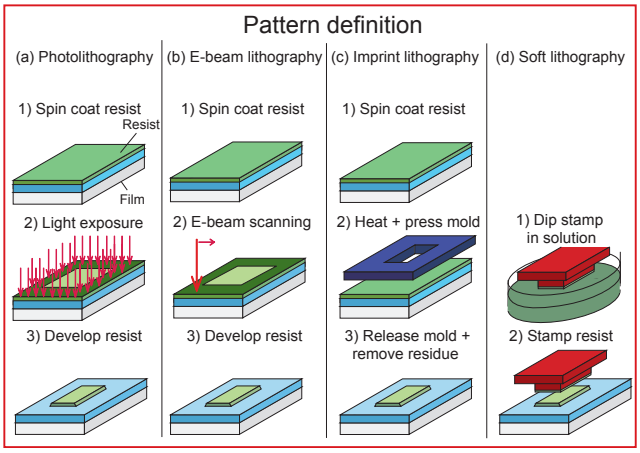

Fig. 2 A resist film can be patterned by for example (a) photolithography, (b) e-beam lithography (EBL), (c) nanoimprint lithography, or (d) soft lithography (also known as microcontact printing). Note that during soft lithography, the substrate is only involved in one step.

sure on the other hand, can be used to create anisotropic etch profiles, and is therefore applied during high resolution patterning.[12] Typically, the substrate potential is lower than the plasma potential, such that the positively charged ions in the plasma accelerate towards the substrate in a directional manner, which ensures the anisotropic nature of the etch process. For reactive plasmas this anisotropic nature is ruled by the so-called ion-radical synergism.[13] The remaining resist layer is stripped during the last step of the patterning process, e.g. by plasma ashing or wet chemistry.

As mentioned, there are several patterning techniques that can be used to define the pattern in the resist layer (See Fig. 2). In photolithography,[14] a resist layer is first spin-coated on the substrate using a solution containing the resist molecules in a solvent. After drying and/or baking to remove the solvent, the resist film is exposed to light through a mask with the desired pattern. The exposed regions undergo a chemical change that affects the solubility in a developing solvent. Depending on the photoresist tone, the exposed or unexposed regions are selectively washed away during the development step. For positive tone resists, the exposed regions are more soluble in the resist development solution, while the unexposed regions are more soluble for negative tone resists.

In EBL, an electron beam is scanned over a surface covered with a resist film according to a predefined pattern, instead of exposing it through a mask.[15] The local exposure to the electron beam causes a chemical change of the resist film. For the rest, it consists of the same steps for resist coating and resist development as employed during photolithography, although with different resist and development chemicals.

Nanoimprint lithography (originally known as hot embossing) involves a hard mold shaped in the preferred pattern that is imprinted in a polymer film.[16] The polymer film is first spin-coated on the substrate and heated. The hard mold is subsequently pressed into the polymer film. When heated above the glass transition temperature of the polymer, the material flows into the structures of the mold. The substrate is then cooled, which causes the polymer to solidify and replicate the pattern of the mold. Finally, the mold is released, and the resist residue is removed in a short etching treatment. Instead of heating the substrate, certain polymers can alternatively be cured when the mold is applied using ultraviolet (UV) light.

Soft lithography (also known as microcontact printing) relies on the stamping of molecules on the substrate.[17] In the first step, an elastomeric stamp is created from a hard master. Subsequently, the elastomeric stamp is put into contact with the molecules. The 'inked' stamp is then placed on the substrate, and the molecules are transferred to the substrate surface by applying a force on the stamp.

Photolithography and etching are well-established processing techniques in the microelectronics industry, while EBL, soft lithography and imprint lithography are frequently employed in research environments. The technique used for film deposition does normally not affect the subsequent pattern definition and etching processes. Therefore, there is no literature specifically about the patterning of ALD-grown films with conventional methods. It can however safely be stated that patterning based on etching is the most adopted way of structuring these films for various applications.

Conventional patterning can be classified as subtractive, top-down, processing, in which blanket films are deposited first, and the structuring is performed by etching. For certain applications, etch steps are unacceptable since they may damage sensitive elements of the structure. For example etching needs to be avoided on organic semiconductors,[18,19] or on carbon-based materials such as carbon nanotubes or graphene. Another limitation is that some metals such as Cu, Pd, Pt, Ag, and Au are difficult to etch by dry etching.[20] The alternative is to deposit the material only on those areas where it is desired, using lift-off approaches or area-selective deposition, as explained in Sec. IV.

The resolution that can be achieved with photolithography is limited by the wavelength of the light that is used. The resolution of photolithography has been improved during the past few decades by using light of increasingly shorter wavelengths (from 436 nm in 1980 to 193 nm currently), with extreme ultraviolet (EUV) light (13.6 nm) as the future candidate for high-volume manufacturing in microelectronics. The next section describes how the lithography process can be adapted to fabricate features with a higher resolution without using light of a shorter wavelength.

III. ALD-enabled nanopatterning

A. Spacer defined double patterning

Lithography tools currently use UV light with a wavelength of 193 nm. By immersion of the gap between the lens and the wafer surface in purified water (i.e. in immersion lithography),[21] these tools allow for the patterning with a critical dimension around 40 nm.[11] To increase the resolution further, light of a shorter wavelength has to be used, or alternatively, new resolution enhancement technologies must be employed. Since the transition to EUV lithography turns out to be challenging for high-volume manufacturing, several double exposure and double patterning approaches are currently being developed and implemented.[22] These approaches allow for the use of the current lithography tools for a few more years, which is beneficial from a cost-of-ownership point-of-view.

The most straightforward way to increase the resolution is to perform two lithography steps on the same resist, referred to as double exposure (See Fig. 3a).[23] Standard resist films suffer however from a memory effect: the sum of two times a subthreshold dose at locations in proximity to the exposed regions may be higher than the threshold for making the resist soluble,[24] which widens the dimensions of the patterned features. The implementation of double exposure therefore requires the use of a new class of resist films with a nonlinear response to the exposure dose.

Alternatively, a double patterning approach can be used in which both exposure steps are followed by separate resist development and etching steps.[24] However, the limitations of double patterning are that it involves many processing steps, and that the wafer has to be removed from the lithography tool for the additional resist development, etching, and resist coating steps, which causes loss of overlay registration.

A modified double patterning approach that involves only one lithography step, and therefore no additional challenges with respect to overlay, is spacer defined double patterning (SDDP).[25] Because photolithography is normally the limiting step in integrated circuit manufacturing (due to the high capital expenditure of lithography equipment), it is a major improvement when a higher patterning resolution can be achieved without performing two exposures. As illustrated in Fig. 3b, SDDP starts with the deposition of a hard mask and a resist film on top of the film that needs to be structured. The resist film is patterned by photolithography, which is followed by the development of the resist. The pattern is then transferred into the hard mask using anisotropic etching. After the removal of the resist, a spacer layer is deposited on the patterned hard mask by using for example plasma-enhanced chemical vapor deposition (PECVD) or ALD. It is important that a uniform and conformal spacer layer is deposited in this step, especially

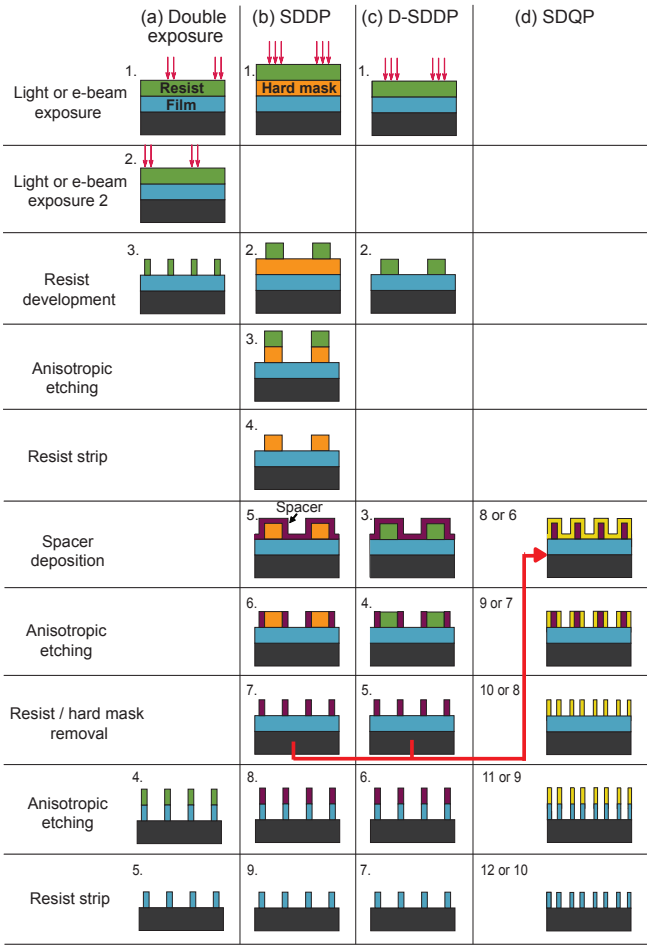

Fig. 3 Overview of the process flows of different resolution enhancement approaches: (a) double exposure, (b) spacer defined double patterning (SDDP), (c) direct spacer defined double patterning (D-SDDP), and (d) spacer defined quadruple patterning (SDQP). The first steps of SDQP are the same as the first 7 steps of SDDP or the first 5 steps of D-SDDP.

when increasingly small features need to be patterned. This motivates the implementation of ALD in SDDP fabrication schemes, since ALD is a technique with unparalleled capabilities for the deposition of conformal films on demanding surfaces.[2] The thickness of the spacer layer needs to equal to the targeted critical dimension.[11] Subsequently, a second etch is performed to remove the spacer layer covering the top of the hard mask. This needs to be done such that the sidewalls of the spacer layer remain intact; for example using reactive ion etching (RIE). In addition, also the rest of the hard mask needs to be etched away, using a etching process that is selective towards the hard mask material. This leaves the sidewalls of the spacer layer behind. The half-pitch is now reduced because both sidewalls define a feature. The pattern is subsequently

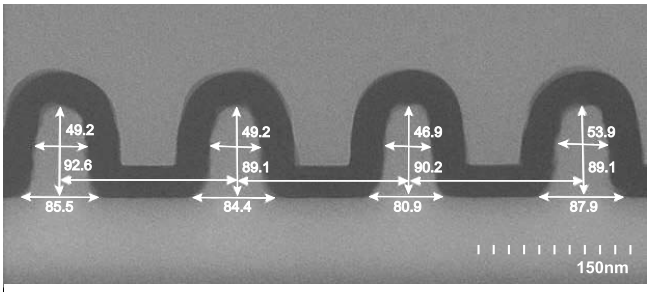

Fig. 4 Scanning electron microscopy (SEM) image of a patterned photoresist covered with a SiO_2 spacer layer deposited by plasma-assisted ALD at 50 °C. Courtesy of ASM International N.V.

transferred to the target film by anisotropic etching, in which the spacer layer sidewalls function as the mask. In the last step, the spacer layer is also removed by etching. The final result is a pattern with twice as much features and a smaller critical dimension as compared to the pattern defined by photolithography in the resist film during step 1.

The procedure of SDDP includes the deposition and patterning of the hard mask layer, because typical polymer resists cannot withstand the temperature required for the deposition of the spacer layer by conventional techniques such as plasma-enhanced chemical vapor deposition (PECVD). This implies that when the spacer layer could be deposited directly on the patterned photoresist (referred to as direct spacer defined double patterning, D-SDDP), several processing steps can be eliminated as illustrated in Fig. 3c.[9,26,27] ALD, and in particular plasma-assisted ALD, allows for the deposition of a high-quality spacer layer at low substrate temperatures.[10,11] There are several low temperature ALD processes that could be suitable for the deposition of the spacer.[28,29] It is important that the spacer layer is coated conformally on the patterned resist film in the D-SDDP approach (See Fig. 4), which is a second reason to use ALD instead of PECVD.

The patterning of 32 nm half-pitch polysilicon lines by D-SDDP with a SiO_2 spacer layer deposited by plasma-assisted ALD has been achieved by Beynet *et al.*[9] Some other studies also report the use of ALD-grown SiO_2 as spacer layer in SDDP,[30–32] while there is also interest in Si-containing ternary compounds.[33] In addition, ALD-enabled SSDP has been used by Dhuey *et al.* to fabricate nanoimprint template gratings with 10 nm half-pitch.[34] In that work, EBL was employed to define the initial features, and D-SDDP involving plasma-assisted ALD of Al_2O_3 subsequently allowed for doubling of the spatial frequency of the gratings. In earlier work of the same group, ALD was used to tune the dimensions of nanoprint lithography templates to sub-10 nm resolution,[35] which can also be referred to as ALD-enabled nanopatterning.

The next resolution enhancement technology that may be applied is quadruple patterning.[30,31] After step 7 of SDDP or step 5 of D-SDDP, a second spacer deposition step may be performed, in order to double the resolution once more. Spacer defined quadruple patterning (SDQP) requires a different material for the second spacer layer, such that the first spacer layer can be etched selectively without affecting the second spacer layer material.[11]

B. Resist modification

Another form of ALD-enabled nanopatterning is the use of ALD to modify the properties of resist films. The thickness of resist films for high resolution patterning is limited in photolithography due to the depth-of-focus of the lithography tool, and in EBL because of lateral scattering of electrons.[36] In addition, a thin resist film is also required to avoid pattern collapse during resist development and drying (known as "wet collapse"). On the other hand, a high etch resistance is needed during subsequent etching, which in principle motivates the use of relatively thick resist films. Since it is difficult to satisfy all these requirements, it is often essential to transfer the pattern to a hard mask with a higher etch resistance. Several studies investigated the use of ALD and the related method of sequential infiltration synthesis (SIS) for the enhancement of the etch resistance of various resist films. A first study in this direction was reported by Sinha *et al.*, in which the etch resistance of poly(*tert*-butyl methacrylate) (PtBMA) resist films was enhanced by ALD of a thin TiO_2 layer on top of the resist film.[37]

Tseng *et al.* improved this approach by using long precursor and reactant exposure steps such that the deposited material infiltrates in the porous resist film. In this way, Al_2O_3 was deposited in the bulk of the e-beam resists PMMA and ZEP520A.[38] The ALD technique was referred to in the work as sequential infiltration synthesis (SIS), to stress that long pulse times were chosen. The long pulse times, together with elevated process pressures, enable SIS at low substrate temperatures, which is beneficial for the deposition in polymers.[39] Tseng *et al.* reported an improvement of the etch resistance by a factor of 37 for PMMA and 5 for ZEP520A, and it was discussed that this improved etch resistance eliminates the need for using a hard mask.[38] It was further demonstrated that when SIS is applied to PMMA resist, the aspect-ratio of the resist structures can be decreased below the limit for which wet collapse starts to occur.[36] This SIS-modified PMMA resist already meets the requirements of the International Technology Roadmap for Semiconductors of 2022.[36]

In subsequent work, SIS was also applied to block copolymer (BCP) lithography.[40,41] Block copolymers consist of two chemically different homopolymers connected together through covalent bonds. These BCPs can self-assemble in periodic nanostructures of various shapes (e.g. pillars, sphere,

lamellae) through microphase separation. The shape and size of BCPs can be tuned by selecting homopolymers with specific chemical composition and molecular weight.[42] The application of SIS to BCP lithography builds upon earlier work in which area-selective ALD was performed on BCPs to fabricate a hard mask.[43] Moreover, similar methods have been used extensively to synthesize various nanostructures as discussed in more detail in Sec. VI.E. BCP lithography relies on etching with the periodic structure of a BCP acting as a nanopatterned resist. The main challenge of BCP lithography is that the thickness of a BCP film is on the order of the domain size, which is too thin for an effective etch resist. BCP lithography is therefore limited to the etching of low aspect-ratio structures. A workaround is to transfer the BCP pattern to an intermediate hard mask, but this offers additional complexity and costs. Tseng *et al.* showed that the etch contrast between the PS and PMMA blocks of a PS-*b*-PMMA BCP can be enhanced by Al_2O_3 SIS. The Al_2O_3 is selectively deposited in the PMMA, which increases the etch resistance of the PMMA domains. Various BCP patterns were successfully transferred via plasma etching to the substrate materials Si (See Fig. 5), indium tin oxide (ITO) and permalloy ($Ni_{0.8}Fe_{0.2}$).

Due to its ability to synthesize small nanoscale features of of 5 - 30 nm, BCP lithography schemes have the potential to enable further downscaling of microelectronic devices.[39,44] However, the use of BCP lithography to make a large number of devices is challenging because of the absence of long-range order in BCPs.[42] Therefore, an external driving force is required to change the random morphology of BCPs into an oriented pattern that could be useful for semiconductor processing. For example, in an approach called graphoepitaxy, a nanostructured surface with aligned features (e.g. trenches or bars) is used to orient the BCP formation.[42] See Fig. 5c for an example of a structure created using graphoepitaxy. Alternatively, a chemical pattern on a flat surface can be used to align BCPs. The main BCP scheme that is considered for integrated circuit manufacturing, referred to as directed self-assembly (DSA) lithography, consists of the patterning of features with at large pitch with conventional lithography, followed by the reduction of the pitch by self-assembly of BCPs in between the features. DSA lithography can be described as a combination of top-down (i.e. conventional lithography) and bottom-up (i.e. self-assembly) processing.

Ruiz *et al.* evaluated the processing compatibility of SIS with DSA.[45] EBL and RIE were employed to make a sample with patterned stripes at a pitch of 54 nm providing the chemical contrast for aligned BCP formation.[46] The DSA process was characterized by a density multiplication factor of 2×, meaning that the BCPs aligned in registration to the chemical contrast stripes with a spacing of 27 nm between the lamellae. Three Al_2O_3 SIS cycles were carried out, as this was found to result in an effective hard mask, and well-defined patterns.[45]

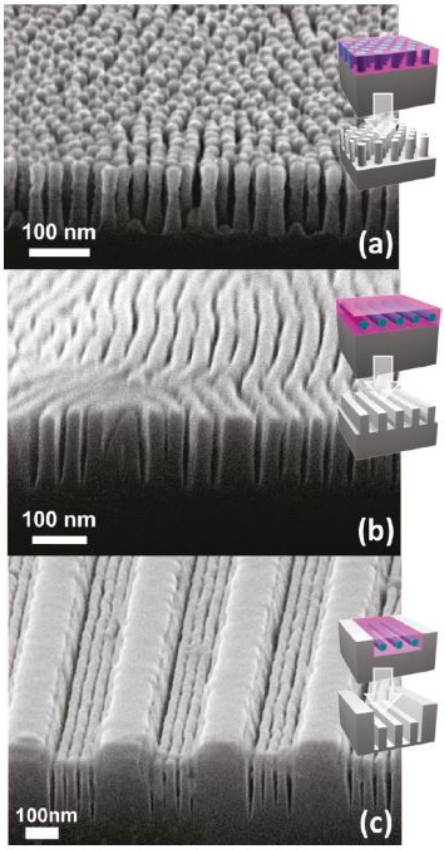

Fig. 5 SEM images of several nanostructures fabricated by plasma etching using SIS-enhanced PS-*b*-PMMA as the etch mask. The PMMA regions were shaped in the form of: (a) standing cylinders, (b) in-plane cylinders, and (c) in-plane cylinders aligned using graphoepitaxy. Reprinted (adapted) with permission from (Y.-C. Tseng *et al.*, *J. Phys. Chem. C*, 2011, **115**, 17725). Copyright (2011) American Chemical Society.

Structures of ∼12 nm size and 27 nm pitch were created, and it was found that these structures have a low line edge roughness of $3\sigma = 2.9$ nm.[45]

IV. Nanopatterning of ALD-grown films

This section reviews the different methods that have been reported for the patterning of ALD-grown films: (*i*) patterning based on lithography and lift-off, (*ii*) area-selective ALD by area-deactivation, and (*iii*) area-selective ALD by area-activation.

A. Patterning based on lithography and lift-off

In lift-off methods, the material is deposited after the patterning of the resist. As illustrated in Fig. 6b, the process flow for

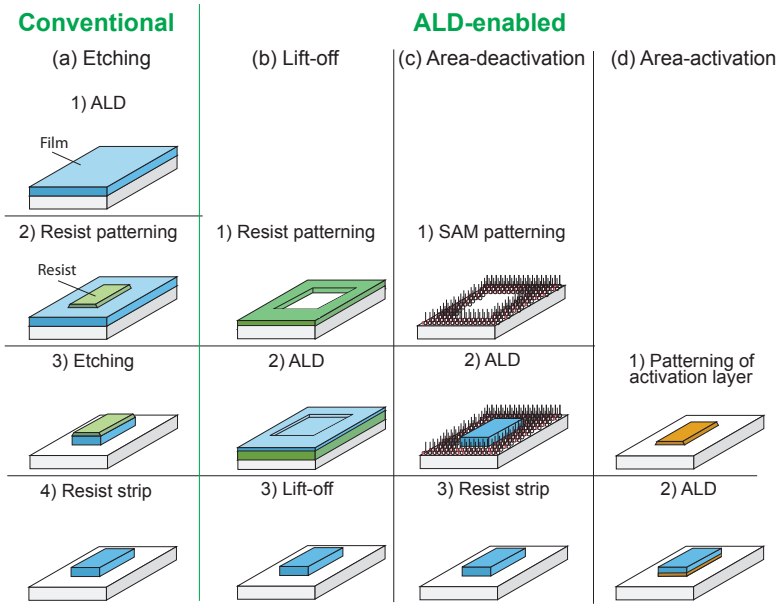

Fig. 6 Schematic representations of the typical process flows in (a) conventional patterning based on lithography and etching, (b) patterning based on lithography and lift-off, (c) area-selective ALD by area-deactivation, and (d) area-selective ALD by area-activation. Approaches (b,c,d) can be classified as *ALD-enabled nanopatterning*. Approaches (a,b,c) include several additional processing steps for the patterning of the resist film or SAM (See Fig. 2).

lift-off patterning is very similar to the conventional patterning scheme illustrated in Fig. 6a. However, the main difference is that the etching step is eliminated. The first few steps consist of the patterning of a resist film using for example one of the patterning techniques described in Sec. II. The resist is thereby applied in the areas, where the deposition of material needs to be prevented. Subsequently, the film is deposited on the entire surface of the substrate. The deposited film covers the parts of the substrate where no resist is present as well as the top of the resist layer. In the actual lift-off step, the resist layer is dissolved and washed away together with the material that was covering the resist. The targeted material stays only on those areas where the material is in direct contact with the substrate.

As discussed in Sec. II., lift-off patterning is typically applied when etching would damage parts of the device structures, or when processing materials that are difficult to etch. Similar to lithography and etching, lift-off patterning is a widely used approach in the microelectronics industry. Consequently, for most resist films and materials, information is available in the literature about how to perform a successful lift-off.

A general limitation of lift-off approaches is that the material needs to be deposited at a relatively low temperature such that the resist film stays intact.[3] The deposition of films by ALD is interesting for lift-off patterning, because it typically allows for the deposition at substrate temperatures lower than the temperature that is required for chemical vapor deposition (CVD) processes.

Several articles in the literature deal with the use of lift-off patterning for the structuring of ALD-grown films as listed in Table 1. Biercuk *et al.* reported on the fabrication of dielectric structures of Al_2O_3, HfO_2 and ZrO_2.[3] Patterning was performed by photolithography using Shipley photoresist and by EBL using PMMA resist. The films were deposited at low substrate temperature (100 - 150 °C), to prevent significant outgassing or hardbaking of the resist layers. The lift-off step was performed by immersing the samples in acetone. Structures with film thicknesses in the range 2.5 - 100 nm and submicron lateral resolution were fabricated.

In a study by Suresh *et al.*, illustrated in Fig. 7, patterned ZnO was prepared in a lift-off approach using nanoimprint lithography (Fig. 2c) as the patterning technique.[50] A mold with a periodic pattern of Si nanopillars of 65 nm in diameter was used in a standard nanoimprint lithography process in which PMMA was patterned on the substrate. After removal of the residual layer by an O_2 plasma, ALD of ZnO was carried out at a substrate temperature of 70 °C. Finally, a lift-off step was conducted using acetone. This procedure resulted in a periodic array of ZnO structures of which metal-oxide-semiconductor (MOS) capacitors were fabricated.

Although referred to as area-selective ALD, the work of Sinha *et al.* about TiO_2 deposition from $TiCl_4$ and H_2O can be classified as a lift-off patterning since also deposition on

Table 1 Overview of studies reported in the literature about nanopatterning based on lithography and lift-off. The material deposited, the precursors used for ALD, the temperature during ALD, the resist film, the patterning technique, and the thickness and the lateral size of the final pattern are given. The smallest reported lateral dimension of a patterned structure is listed as a measure for the resolution. A tilde indicates that a value is not presented in the article but is estimated from the reported data instead, and a dash means 'not reported'. Me = methyl, Et = ethyl, CpAMD = cyclopentadienyl isopropyl acetamidinato, PMMA = poly(methylmethacrylate), PVP = poly(vinyl pyrrolidone).

Material	Precursors	Temp.	Resist	Patterning	Thickness	Lateral	Refs.
		(°C)			(nm)	(μm)	
Al_2O_3	$Al(Me)_3 + H_2O$	100 - 150	PMMA	EBL	-	-	3
		250	PMMA	Photolitho.	50-380	60	47
			PVP	Photolitho.	-	$\sim$50	48
	$AlCl_3 + H_2O$	250	PMMA	Photolitho.	40	55	47
			PVP	Photolitho.	39	$\sim$50	48
TiO_2	$TiCl_4 + H_2O$	160	PMMA	Photolitho.	$\sim$11	$\sim$50	49
ZnO	$ZnEt_2 + H_2O$	70	PMMA	Imprint	13	55	50
		200	PMMA	Photolitho.	98	$\sim$20	51
ZrO_2	$Zr(NMe_2)_4 + H_2O$	100 - 150	PMMA	EBL	-	-	3
	$ZrCl_4 + H_2O$	250	PVP	Photolitho.	80	$\sim$50	48
HfO_2	$Hf(NMe_2)_4 + H_2O$	100 - 150	-	Photolitho.	-	-	3
			PMMA	EBL	15	80 nm	3
CeO_2	$Ce(thd)_4 + O_3$	200	Ag	EBL	-	0.6	52
Co	Co(CpAMD) + NH_3 plasma	100	AZ-5214	Photolitho.	-	$\sim$50	53

the top of the PMMA resist was obtained.[49] The deposition on the resist was reduced as much as possible by prolonging the purge times. The reduced growth of TiO_2 on the PMMA resist facilitates the lift-off step. In an another study, Sinha *et al.* observed that when titanium isopropoxide ($Ti(O^iPr)_4$) is used as the precursor for TiO_2 deposition instead, no growth on the PMMA resist occurs.[54] That study is listed as area-selective ALD by area-deactivation in Table 3. To explain the difference between the two TiO_2 ALD processes, the transport behavior of water, $TiCl_4$, and $Ti(O^iPr)_4$ through various polymer resist films was investigated in a follow-up study.[55] It was observed that a negligible amount of water adsorbs in polymer masking layers, while a significant difference between the diffusion coefficients of $TiCl_4$, and $Ti(ipr)_4$ was measured.

Färm *et al.* demonstrated successful lift-off patterning of Al_2O_3 and TiO_2 with 100 nm thick PMMA at 250 °C.[47] This temperature is well above the glass transition temperature of PMMA, i.e. 85 - 165 °C (depending on the exact properties of the PMMA used). The use of temperatures above this range leads to hardening of the resist, which makes the lift-off step difficult. Note however, that only structures with dimensions larger than $\sim$50 μm were successfully synthesized. Patterning nanoscale structures was also attempted, but failed for temperatures above 150 °C.[48]

A complicated lift-off procedure was employed by Coll *et al.* to enable the patterning of CeO_2 structures.[52] CeO_2 ALD from $Ce(thd)_4$ precursor requires ozone as the reactant and a substrate temperature above 200 °C, which is not compatible with the use of organic polymers. Therefore, a Ag layer was patterned as a lift-off layer using EBL, which was followed by CeO_2 ALD. Subsequently, the Ag was etched away in HNO_3 solution, leaving the CeO_2 structures behind.

Kim *et al.* reported the only study in which plasma-assisted ALD was used in lift-off patterning.[53] Microscale structures of Co were fabricated using an ALD process involving Co(CpAMD) precursor and NH_3 plasma. Plasma-assisted ALD was required to allow for the deposition of Co at a low substrate temperature such that the resist film stays intact during ALD.

In principle, the lift-off step for an ALD-grown film should be similar to the lift-off step for films deposited by other means. However, due to the excellent conformality of ALD, growth in porous polymers can be obtained,[49] which makes the lift-off step more challenging. For the same reason, it may be more difficult to avoid the deposition on the sidewalls of the resist. These issues lower the device yield when a wafer with a large multitude of devices needs to be fabricated, and make it extremely challenging to pattern with a high resolution. To date, the patterning of fine features of $<$100 nm in a lift-off approach using ALD has not been demonstrated. A solution to these issues is to modify the method such that the growth on the patterned resist film is avoided, as is the case for area-selective ALD by area-deactivation.

B. Area-selective ALD by area-deactivation

As mentioned in the Introduction, ALD depends strongly on surface chemistry, and can therefore be limited to a part of the substrate by locally modifying the surface properties. For metal-oxides for example, the nucleation starts in most cases

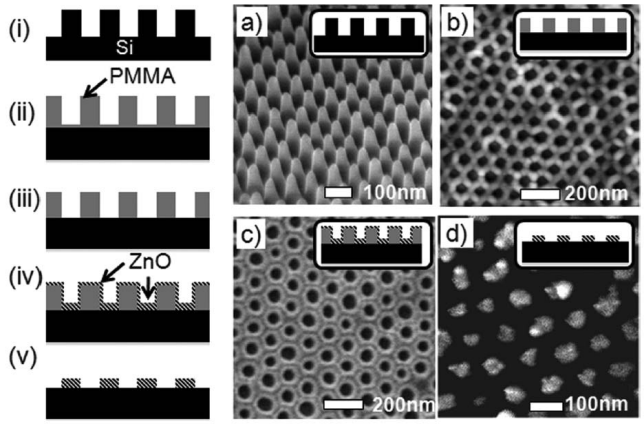

Fig. 7 The method developed by Suresh *et al.* for the fabrication of a periodic pattern of ZnO: (*i*) Mold fabrication from Si; (*ii*) Nanoimprint lithography; (*iii*) Removal of the residual layer; (*iv*) ALD of ZnO; and (*v*) Lift-off. The SEM images in (a) and (c) show the mold and the surface after steps (*i*) and (*iv*), respectively. The AFM images (b) and (d) show the surface after steps (*iii*) and (*v*), respectively. Reprinted (adapted) with permission from (V. Suresh *et al.*, *J. Phys, Chem. C*, 2012, **116**, 23729). Copyright (2012) American Chemical Society.

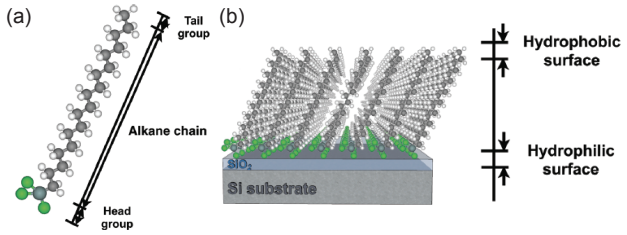

Fig. 8 Schematic representation of (a) an octadecyltrichlorosilane (ODTS) molecule, and (b) a SiO_2 surface covered with an ODTS SAM. The SAM transforms the hydrophilic SiO_2 surface to a hydrophobic surface terminated with -CH_3 groups. From Ref. 4. Copyright © 2012 Wiley-VCH Verlag GmbH & Co. KGaA.

readily on a hydrophilic OH-terminated surface, while there is a short nucleation delay of a few cycles on hydrogen-terminated[56,57] or metal surfaces.[58] On the other hand, it has been reported that the (^{t}Bu-Allyl)$Co(CO)_3$ precursor for Co ALD is more reactive with H-terminated surfaces than OH-terminated surfaces.[59] This suggests that area-selective ALD can for example be obtained by patterning OH-terminated areas on a hydrogen-terminated surface prior to the ALD growth. However, due to the small difference in nucleation delay, the growth remains selective to the OH-terminated areas for only a few cycles, and only an extremely thin pattern can be fabricated that way. In practice, it is required to deactivate specific areas of the substrate by molecules that are more effective in preventing ALD growth.

The majority of approaches for achieving area-selective ALD reported in the literature rely on the deactivation of the surface by self-assembled monolayers (SAMs). Typically, these SAMs are made of long organic molecules with reactive groups at both ends of the molecules. Figure 8 illustrates that such a molecule consists of three elements: the head group, an alkane chain as the backbone, and a tail group. The head group facilitates the binding of the molecule to the surface. Van der Waals interactions between the alkane chains contribute to the formation of an ordered monolayer of molecules. The surface is terminated with tail groups, when a nicely ordered monolayer is formed. The surface properties can therefore be modified by using molecules with an appropriate tail group. For example, adsorption of octadecyltrichlorosilane (ODTS) molecules with methyl (-CH_3) tail groups on an oxide substrate transforms the surface from an OH-terminated hydrophilic surface to a CH_3-terminated hydrophobic surface (Fig. 8). Area-selective ALD is obtained by partly covering the surface with a SAM and subsequently performing ALD. The ALD growth then selectively takes place on those areas that are not covered with the SAM-molecules. Figure 9 illustrates an area-selective ALD process for the deposition of HfO_2 structures.[60] The surface was first patterned with oxide regions on a hydrogen-terminated Si surface by photolithography. The ODTS molecules selectively adsorbed to the OH-terminated oxide areas, and area-selective ALD of HfO_2 was obtained on part of the surface not covered with the ODTS molecules.

In contrast to conventional nanopatterning approaches, area-selective ALD is an additive approach, in which the material is only deposited at those areas where it is desired. The difference with lift-off methods is that the growth in deactivated areas is blocked in a chemical way, instead of by physically masking the surface. In principle, no growth takes place at the top of the SAM, and it is therefore also relatively straightforward to remove the SAM after the deposition of the material. The main advantages of area-selective ALD as compared to conventional patterning approaches is that it involves less processing steps (See Fig. 6). However, this is only the case if the patterning is performed with for example microcontact printing, instead of by multi-step photolithography.

Table 2 shows an overview of the literature reports on area-selective ALD relying on area-deactivation by SAMs. Successful area-selective ALD has been achieved for many different materials, including metal-oxides, metal-sulfides, and metals. Note that only thermal ALD processes with H_2O, O_2, NH_3, and H_2S as the reactant are listed, which reflects the fact that plasmas or ozone can destructively react with organic SAM molecules. Lee *et al.* investigated whether area-selective ALD of Co can be obtained on an ODTS patterned surface by plasma-assisted ALD from Co(^{i}Pr-AMD)$_2$ and NH_3 plasma.[79] It was found that a surface covered with a

Table 2 Overview of studies reported in the literature about area-selective ALD by area-deactivation using SAMs. The material deposited, the precursors used for ALD, the temperature during ALD, the SAM, the patterning technique, and the thickness and the lateral size of the final pattern are given. The smallest reported lateral dimension of a patterned structure is listed as a measure for the resolution. A tilde indicates that a value is not presented in the article but is estimated from the reported data instead, and a dash means 'not reported'. O^iPr = isopropoxide, Me = methyl, Et = ethyl, ^{t}Bu = *tert*-butyl, thd = 2,2,6,6-tetramethyl-3,5-heptanedionato, ^{i}Pr-AMD = bis(*N*,*N*'-diisopropylacetamidinato), dmamb = bis(dimethylamino-2-methyl-2-butoxy), Cp = cyclopentadienyl, acac = acetylacetonate, ODT = octadecanethiol, ODTS = octadecyltrichlorosilane, ODS = octadecyltrimethoxysilane, DTS = docosyltrichlorosilane, ODPA = octadecylphosphonic acid, PDIC = 1,4-phenylenediisocyanate, ED = ethylenediamine, RT = room temperature, μCP = microcontact printing.

Material	Precursors	Temp.	SAM	Patterning	Thickness	Lateral	Refs.
		(°C)			(nm)	(μm)	
TiO_2	$Ti(O^iPr)_4 + H_2O$	100	ODT	μCP	15	0.5	61
		150	ODTS	EBL	~2	20 nm	62
			ODTS	μCP	2	570 nm	63
	$Ti(OMe)_4 + H_2O$	250	ODTS	μCP	7	1.5	64
ZnO	$ZnEt_2 + H_2O$	125	DTS	μCP	60	1	65
		150	ODPA	-	19	50	66
ZrO_2	$Zr(NMe_2)_4 + H_2O$	200	ODTS	AFM	7	40 nm	67
	$Zr(OCMe_3)_4 + H_2O$	-	ODTS	Photocatal.	~16	430 nm	68
HfO_2	$Hf(O^tBu)_4 + H_2O$	200	ODTS	Self-assembly	3	9 nm	69
	$Hf(NMe_2)_4 + H_2O$	-	ODTS	Photolitho.	~5	5	60,70
			ODTS	μCP	4	~30	17
PbS	$Pb(thd)_2 + H_2S$	160	ODTS	Photolitho.	4.5	~3	71
				AFM	4.5	40 nm	71
Co	$Co(^i$Pr-AMD$)_2 + NH_3$	350	ODTS	Photolitho.	24	3	72
Ni	$Ni(dmamb)_2 + NH_3$	300	ODTS	Photolitho.	~55	3	73
Ru	$RuCp_2 + O_2$	325	ODTS	μCP	~15	100	74
Ir	$Ir(acac)_3 + O_2$	225	ODS	Lift-off	22	50	75
			ODTS	μCP	23	1.5	64
		250	1-dodecanethiol	-	-	-	76
Pt	$MeCpPtMe_3$ + air	285	1-octadecene	Photolitho.	2.5	~5	70
		285	ODTS	μCP	3	2	17,77
Polyurea	PDIC + ED	RT	ODTS	μCP	6	~2	78

hydrophobic ODTS SAM transformed into a completely hydrophilic surface after 50 s NH_3 plasma, and as a result, the growth was not selective. Recently, also an organic polyurea film has been patterned using area-selective molecular layer deposition (MLD).[78]

Several SAMs have been used for achieving area-selective ALD. The table only lists those SAMs for which successful area-selective ALD was reported. In addition, several other SAM molecules have been investigated for their ability to deactivate ALD growth.[6,80–82] Most of the SAM molecules in Table 2 are chlorosilanes with -$SiCl_3$ as the head-group. This is because these molecules easily adsorb at a (native) oxide film on a Si substrate, which is very commonly used in microelectronics applications. Chen and Bent demonstrated that several 1-alkynes and 1-alkenes molecules are also suitable for forming SAMs on Ge substrates.[82] All molecules listed in Table 2 have -CH_3 as the tail group, as this group is very effective in deactivating ALD growth.[83] The length of the alkane chain is important for obtaining an ordered SAM, because it determines the van der Waals forces between the SAM molecules. Chen *et al.* showed that an alkane chain length larger than 12 units is required to block HfO_2 ALD completely.[81] Alternatively, certain SAM molecules have the ability to stimulate ALD growth,[84,85] which can also be exploited for area-selective ALD as illustrated in Fig. 10.[61]

The table also shows that various techniques have been employed for the patterning of SAMs. Microcontact printing (μCP) / soft lithography (See Fig. 2d) is the most popular method, because it is an inexpensive and straightforward approach for patterning an organic layer.[17] The choice for a certain patterning technique determines the complexity of the overall approach. For example, photolithography involves many more processing steps than microcontact printing (See Fig. 1).

The resolution that can be achieved for structures created by area-selective ALD depends mostly on the patterning technique employed. Structures with dimensions of several micrometers have been fabricated using microcontact printing.

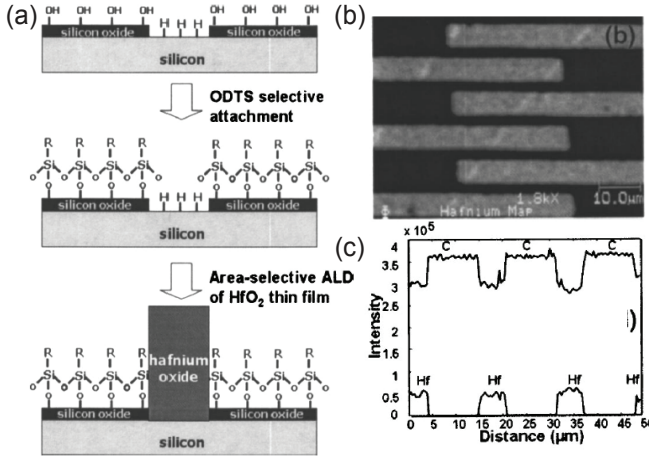

Fig. 9 (a) Area-selective ALD of HfO_2 relying on local deactivation of the growth by an ODTS SAM. The surface was patterned with oxide regions using conventional photolitography. The ODTS molecules selectively adsorbed on the hydroxyl groups present in the oxide regions, and area-selective ALD of HfO_2 was obtained on the regions not covered by the SAM. (b,c) Results from Auger electron spectroscopy (AES) analysis. Reprinted with permission from [R. Chen *et al.*, *Appl. Phys. Lett.*, 2005, **86**, 191910]. Copyright [2005], AIP Publishing LLC.

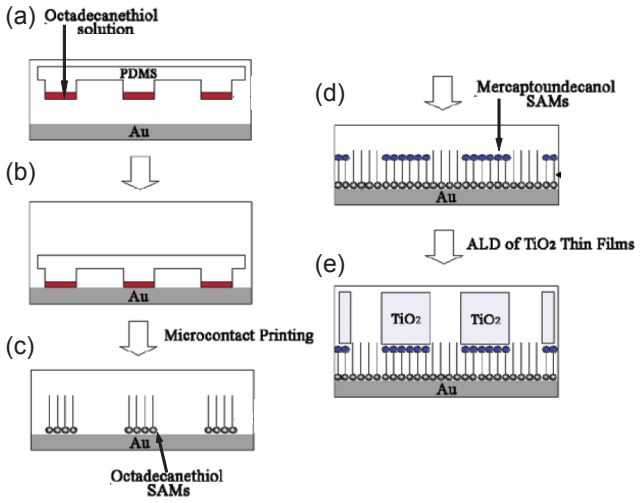

Fig. 10 (a-e) Schematic representation of the approach of Seo *et al.* for the patterning of TiO_2 using microcontact printing of a octadecanethiol (ODT) SAM on Au, followed by area-selective ALD. After the printing of the patterned ODT monolayer, the surface was exposed to mercaptoundecanol SAM molecules in step (d) to locally stimulate the TiO_2 ALD. Reprinted (adapted) with permission from (E. K. Seo *et al.*, *Chem. Mater.*, 2004, **16**, 1878). Copyright (2004) American Chemical Society.

Lee and Prinz synthesized ZrO_2 structures as small as 40 nm using an AFM for the patterning of the SAM.[67] An ODTS monolayer was locally oxidized using an AFM tip, and area-selective ALD was carried out after the removal of the oxide in diluted HF.[67] In a study by Huang *et al*, nanolines with 20 nm diameter were obtained by electron beam lithography (EBL) in an ODTS SAM and subsequent ALD of TiO_2.[62] The highest resolution of 9 nm was achieved by Liu *et al.* by combining self-assembly of S-layer proteins and area-selective ALD of HfO_2.[69] The S-layer proteins assembled on a Si substrate in a two-dimensional periodic pattern with pores of approximately 9 nm in diameter, and ODTS molecules were selectively adsorbed on these protein units. Subsequently, ALD of HfO_2 was carried out, which resulted in selective growth in the pores, and the ODTS-modified S-layer protein nanotemplate was removed by thermal annealing.[69]

Instead of by SAMs, growth for certain ALD processes can also be prevented by polymer films. For example, by those films typically used as resist films in lithography-based approaches. Depending on whether the ALD film nucleates on the polymer film or not, the patterning method is referred to as lift-off, or as area-selective ALD by area-deactivation. PMMA and PVP were used by Färm *et al.* to pattern ALD films of Al_2O_3[47,48] and ZrO_2[48] in a lift-off approach, as listed in Table 1 and as discussed in Sec. IV.A. ALD of Ru, Ir, and Pt using the same resists did not yield growth on the resist layers, and can therefore be listed as area-selective ALD.[47,48] The benefit of area-selective growth is that no lift-off step is required; only the polymer films needs to be dissolved in the last step of the approach. Table 3 shows an overview of reported area-selective ALD approaches relying on area-deactivation using polymer films.

Levy *et al.* employed inkjet printing to pattern polymer resist films for area-selective ALD.[86] Spatial ALD was carried out instead of conventional (temporal) ALD, which allows for ALD at atmospheric pressures and with a much higher throughput.[51,87] In recent work, thin-film transistors were fabricated by processing a stack of Al_2O_3-doped ZnO (AZO) as source/drain electrodes, Al_2O_3 as gate dielectric, and nitrogen-doped ZnO as channel material.[86] Each layer was separately patterned by printing polyvinyl pyrrolidone (PVP) ink, followed by deposition of the material by spatial ALD, and removal of the PVP with a short O_2 plasma treatment. The results for N-doped ZnO are listed as area-selective ALD by area-deactivation in Table 3 and not as patterning by lift-off, because it was tested that PVP inhibits the ALD growth of ZnO for at least 2000 cycles.[86] No detailed information was given for area-selective ALD of Al_2O_3 using PVP.

There are several challenges for area-selective ALD relying on area-deactivation. Thermal stability of the SAM or polymer film is an important aspect. For area-selective ALD of Pt at 300 °C, it was observed that the ability of ODTS molecules

Table 3 Overview of studies reported in the literature about area-selective ALD by area-deactivation using polymer / photoresist films. The material deposited, the precursors used for ALD, the temperature during ALD, the resist film, the patterning technique, and the thickness and the lateral size of the final pattern are given. The smallest reported lateral dimension of a patterned structure is listed as a measure for the resolution. A tilde indicates that a value is not presented in the article but is estimated from the reported data instead, and a dash means 'not reported'. O^{i}Pr = isopropoxide, Me = methyl, Cp = cyclopentadienyl, thd = 2,2,6,6-tetramethyl-3,5-heptanedionato, Et = ethyl, acac = acetylacetonate, PMMA = poly(methylmethacrylate), PVP = poly(vinyl pyrrolidone), PMAM = polymethacrylamide, μCP = microcontact printing.

Material	Precursors	Temp.	Resist	Patterning	Thickness	Lateral	Refs.
		(°C)			(nm)	(μm)	
TiO_2	$Ti(O^iPr)_4 + H_2O$	140	PMMA	AFM	2	~6	88
		160	PMMA	Photolitho.	35	~100	54
	$Ti(OMe)_4 + H_2O$	250-275	PMMA	Photolitho.	25	33	47
CeO_2	$Ce(thd)_2 + O_3$	200	Shipley S1813	μCP	1.5	10	89
N-doped ZnO	$ZnEt_2 + (H_2O+NH_3)$	200	PVP	Inkjet	200	70	86
Ru	$RuCp_2$ + air	300-350	PMMA	Photolitho.	41	50	47
		300	PVP	Photolitho.	20	~50	48
Rh	$Rh(acac)_3 + O_2$	300	Photoresist	Photolitho.	~30	-	90
Ir	$Ir(acac)_3 + O_2$	250-300	PMMA	Photolitho.	29	54	47
			PVP	Photolitho.	17	~50	48
Pt	$MeCpPtMe_3 + O_2$	300	PMMA	Photolitho.	71	36	47
			PVP	Photolitho.	24	~50	48
	$MeCpPtMe_3$ + air	280-300	PMAM	μCP	~5	2	91

to deactivate the ALD growth degrades after 400 cycles,[77] and growth on the ODTS monolayer was obtained. This limits the thickness of the pattern that can be created. Moreover, plasma-assisted or ozone-based ALD processes can generally not be used for area-selective ALD, because the plasma or ozone gas enhances the degradation of the SAM / polymer film.[79] An exception is the recent study of Coll *et al.*, in which successful area-selective ALD was carried out for CeO_2 from $Ce(thd)_4$ and O_3 using Shipley S1813 resist.[89]

Furthermore, it is essential to have a defect-free SAM for effective blocking of the ALD growth. The formation of a SAM with almost no defects is not straightforward, and it generally takes more than 24 hours to form a well-packed SAM by immersion of the sample in a solution, or by vapor deposition.[6,17,80] When the SAM preparation time is too short, small nanoparticles are deposited at defects in the SAM, i.e. at locations where the packing density of the SAM molecules is low ("pinholes").

Another challenge is the control of the dimensions of the pattern. In particular for area-selective ALD approaches involving SAMs, it is challenging to fabricate fine features thicker than a few nanometers. A typical SAM is only ~2 nm thick. This implies that features also laterally broaden (See Fig. 11a) once the film thickness exceeds the height of the SAM. In an attempt to synthesize features with lateral dimensions smaller than the film thickness, Ras *et al*. performed ALD of ZnO on the wings of a cicada insect.[92] These wings served as a template consisting of bottle-shaped nanopillars coated with a waxy layer. The growth only occurred in between the pillars, because the pillars functioned as a physical barrier that prevents lateral broadening. Unfortunately, this approach does not provide a solution for the fabrication of similar features on a flat substrate. Thicker films can be deposited without lateral broadening when using a polymer film as the deactivation layer, since these films are typically more than 100 nm thick.

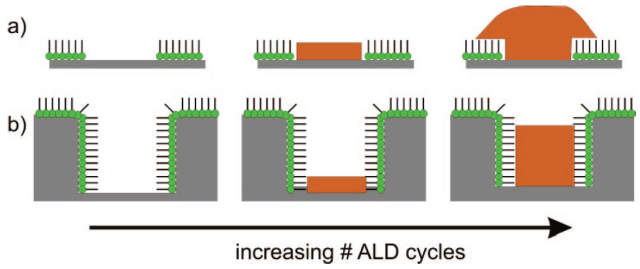

Fig. 11 Area-selective ALD (a) on a surface partially covered with a SAM, and (b) on a wing of a cicada insect. In (a) lateral broadening of the structure occurs when the film thickness exceeds the thickness of the SAM. In (b) there is a physical barrier preventing lateral broadening, and the growth on the wall is deactivated by a waxy layer. Reprinted (adapted) with permission from (R. H. A. Ras *et al.*, *J. Am. Chem. Soc.*, 2008, **130**, 11252). Copyright (2008) American Chemical Society.

C. Area-selective ALD by area-activation

The alternative approach for achieving area-selective deposition relies on local activation of the ALD growth. This can for example be done by patterning of a seed layer that catalyzes the surface reactions of the ALD process. There are two requirements for obtaining area-selective ALD by area-activation: the growth should occur readily on the seed layer, while the growth on the substrate material needs to be suppressed.

Figure 6 clearly illustrates that area-selective ALD by area-activation is much less complex than other approaches for patterning of ALD films. It involves only two processing steps, i.e. the patterning of the seed layer, and the deposition of the material by ALD. It can be described as *bottom-up* processing, because the material is directly deposited only where it is desired, without the need for additional subtractive processing steps such as etching or lift-off.

The nucleation behavior of Pt ALD from $MeCpPtMe_3$ and O_2 gas is discussed here for explaining area-selective ALD by area-activation. Figure 12a depicts the nucleation behavior of Pt ALD on Al_2O_3 and Pt coated surfaces. It shows that no growth occurs when using a low O_2 pressure of 2 mTorr on a Al_2O_3 substrate.[93] On the other hand, Pt growth was obtained using the same conditions on a Pt seed layer. This seed layer was prepared by plasma-assisted ALD.[94] The differences in nucleation behavior on the Al_2O_3 and Pt surfaces can be explained by the reaction mechanism of the ALD process. The combustion of the precursor ligands during Pt ALD needs to be activated by dissociation of the O_2 molecules into atomic O, which is catalyzed by a Pt film.[95] An Al_2O_3 substrate does not have the ability to catalyze dissociative chemisorption of O_2, and as a result, the growth does not easily start on this surface. For the conditions employed, thermal ALD of Pt is selective towards the surface, i.e. it initiates on surfaces with the ability to catalyze dissociative chemisorption of O_2, while no growth occurs on oxide substrates. A seed layer for activation of thermal ALD growth of Pt can also be deposited by other means than plasma-assisted ALD. This implies that area-selective ALD can be obtained on a patterned seed layer.

As mentioned above, the nucleation on the substrate surface needs to be suppressed to allow for selective ALD growth during many ALD cycles. For Pt ALD it was found that the pressure employed during the O_2 pulse of the ALD cycle is the key parameter controlling the nucleation.[96] Figure 12a reveals that Pt ALD does initiate on Al_2O_3 in case a high pressure of 0.8 Torr is employed during the O_2 pulse. This O_2 pressure dependence is further illustrated in Fig. 12b, which shows the growth delay of Pt ALD on Al_2O_3 and Pt surfaces as a function of the O_2 pressure. An extremely long nucleation delay of more than 1000 ALD cycles occurs on Al_2O_3 for O_2 pressures $< \sim$50 mTorr. The growth on a Pt seed layer already takes

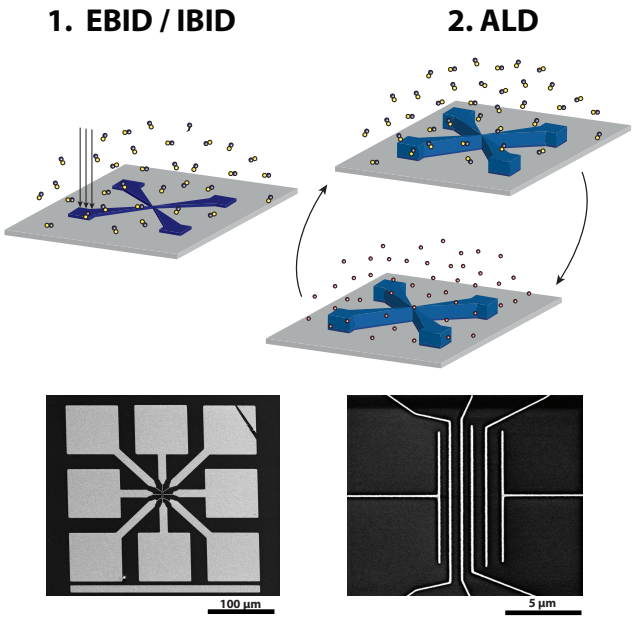

Fig. 13 Schematic representation of the direct-write ALD method, combining electron / ion induced deposition (EBID / IBID) and ALD. The figures below show scanning electron microscopy (SEM) images of structures fabricated with this technique. Reprinted (adapted) with permission from (A. J. M. Mackus *et al.*, *J. Phys. Chem. C*, 2013, **117**, 10788). Copyright (2013) American Chemical Society.

place for an O_2 pressure as low as $\sim$2 mTorr, which indicates that selective growth can be achieved on Pt seed layer patterns for O_2 pressures in the range of 2 mTorr to 50 mTorr.[93]

We have shown that a seed layer can be patterned using the direct-write technique of electron beam induced deposition (EBID)[7,93,97,98] or alternatively by ion beam induced deposition (IBID).[93] The material deposited by EBID or IBID of Pt is of low quality with only 16 - 46 at.% Pt,[99,100] and consists of small Pt grains in amorphous carbon.[101] However, these Pt EBID and Pt IBID seed layers are able to induce Pt ALD growth. In case the ALD growth initiates on extremely thin seed layers, the material is comparable to the quality of ALD films.[93] This approach, referred to as *direct-write ALD*, basically unites the patterning capability of EBID and the material quality of ALD.[7]

Area-selective ALD by area-activation enables patterning with a high lateral resolution. Pt wires with a diameter of $\sim$10 nm have been fabricated by direct-write ALD.[98] The resolution of patterning by area-activation depends solely on the patterning technique used for the deposition of the seed layer pattern, and, for example, not on the properties of a resist film. However, lateral broadening during ALD is expected to occur, similar to what is discussed in Sec. IV.B.

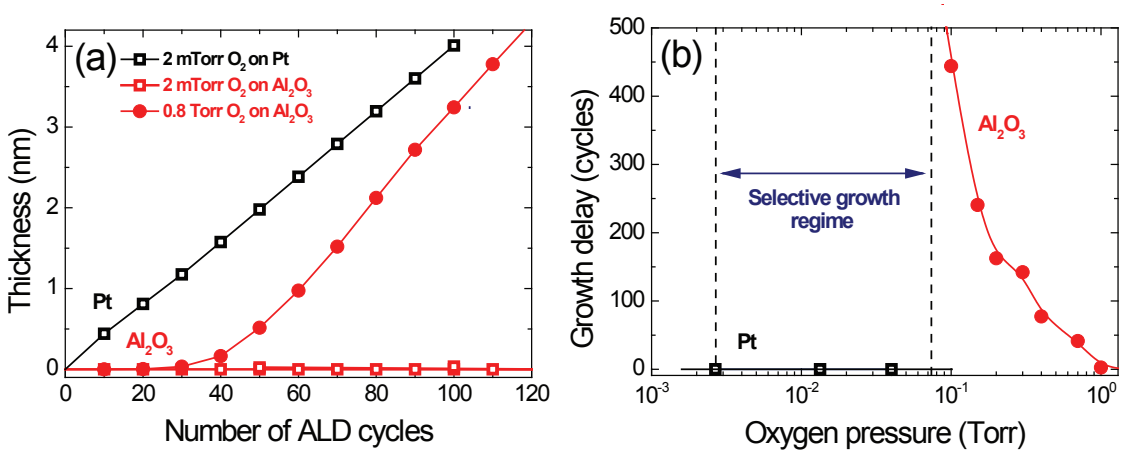

Fig. 12 Graphs illustrating the possibility to perform selective growth of Pt on Pt-containing seed layers. (a) Nucleation curves showing the thickness as a function of the number of cycles for thermal ALD of Pt on Al_2O_3 and Pt coated surfaces. Two different pressures were employed during the O_2 pulse of the ALD process. (b) Growth delay (as deduced from the nucleation curves) as a function of O_2 pressure for thermal ALD of Pt on Al_2O_3 and Pt. The graph defines a regime in O_2 pressure for which the growth is selective on Pt seed layer patterns. Reprinted (adapted) with permission from (A. J. M. Mackus *et al.*, *J. Phys. Chem. C*, 2013, **117**, 10788). Copyright (2013) American Chemical Society.

Table 4 shows an overview of the results reported for area-selective ALD by area-activation. Färm *et al.* proposed an alternative approach for patterning of the seed layer, as well as different conditions to obtain selective growth.[8] Microcontact printing of $RuCl_3$ was used to pattern a RuO_x seed layer for area-selective ALD of Ru. Similar to Pt ALD, the mechanism of Ru ALD depends on dissociative chemisorption of O_2 at the Ru surface.[105,106] To achieve selective growth, they carried out Ru ALD using a lower substrate temperature than is typically employed, in order to reduce the growth on the substrate.[8] Ru ALD from $RuCp_2$ and O_2 has a temperature window of 275 - 400 °C.[107] At 250 °C, growth on a RuO_x seed layer was obtained, and no growth was observed on a Si(100) substrate after 1000 Ru ALD cycles.[8]

The main challenge for area-selective ALD relying on area-activation, is that the nucleation of the ALD process needs to be suppressed on the surface. Therefore, most studies involve metal ALD processes (Cu, Ru, Pd, and Pt) for which the nucleation difficulties on oxides surfaces can be exploited. The development of similar approaches for metal-oxides or metal-nitrides is challenging, since these materials nucleate more easily on most substrates.

The difference in nucleation of TiO_2 from $TiCl_4$ and H_2O on hydrogen-terminated Si and oxidized Si surfaces[108] was recently exploited by McDonnell *et al.* to achieve area-selective ALD by area-activation.[104] It was found that the growth of TiO_2 readily occurs on oxidized Si(111) and Si(100) surface, while only a trace amount of TiO_2 was obtained in case the deposition was carried out on hydrogen-terminated Si. These observations motivated the development of a novel area-selective ALD method relying on scanning tunneling microscopy (STM) tip-based lithography. Patterning was performed by locally stimulating the desorption of bound hydrogen using the STM tip, which led to areas of unpassivated Si. These clean Si areas partly oxidized during the transfer of the samples to the ALD reactor. Subsequently, selective TiO_2 ALD was obtained on those areas where the hydrogen was removed. See Fig. 14 for an AFM image of TiO_2 pattern created using this approach consisting of lines with a diameter of only 15 nm.

To conclude this section, it can be stated that the main merit of area-selective ALD by area-activation is the elimination of many processing steps as compared to conventional patterning, which also mitigates potential compatibility issues. There is no need for etching or lift-off steps, and also the use of resist films or SAMs is eliminated. The latter is for example relevant for the patterning on a carbon nanotubes or graphene, since resists films are generally difficult to remove from carbon-based materials.[109,110]

V. Self-aligned ALD growth

Recently another form of selective ALD growth is gaining attention now that conventional lithography approaches are reaching their limits. In device fabrication, it is often required to deposit a layer on a part of the surface covered with a certain material in the presence of other materials. The standard fabrication procedure would be to perform a multistep lithographic process to pattern the layer on the surface. However,

Table 4 Overview of studies reported in the literature about area-selective ALD by area-activation. The material deposited, the precursors used for ALD, the temperature during ALD, the seed layer, the patterning technique, and the thickness and the lateral size of the final pattern are given. The smallest reported lateral dimension of a patterned structure is listed as a measure for the resolution. A tilde indicates that a value is not presented in the article but is estimated from the reported data instead, and a dash means 'not reported'. thd = 2,2,6,6-tetramethyl-3,5-heptanedionato, Me = methyl, hfac = hexafluoroacetylacetonate Cp = cyclopentadienyl, EBID = electron beam induced deposition, IBID = ion beam induced deposition, μCP = microcontact printing.

Material	Precursors	Temp.	Seed	Patterning	Thickness	Lateral	Refs.
		(°C)			(nm)	(μm)	
Cu	$Cu(thd)_2 + H_2$	190-260	Pt or Pd	-	-	-	102
		235	Pd	Photolitho.	~14	-	103
Pt	$MeCpPtMe_3 + O_2$	300	Pt/C	EBID	-	9 nm	7,98
				IBID	19	5	93
Pd	$Pd(hfac)_2 + H_2$	100	Pt/C	EBID	-	5	98
Ru	$RuCp_2$ + air	250	RuO_x	μCP	29	1.5	8
TiO_2	$TiCl_4 + H_2O$	100	oxidized Si(100)	STM	2.8	15 nm	104

with decreasing device dimensions, and the development of lithography lagging behind, it becomes more and more difficult to achieve a good overlay between the layers. It is therefore more straightforward to deposit the material selectively on those materials where it is desired. This so-called *self-aligned* growth reduces the number of lithographic steps, and eliminates problems with overlay.

Self-aligned chemical vapor deposition (CVD) has been an active topic of research in the early 90s for the fabrication of contacts, interconnects, and diffusion barriers.[111] Many of the investigated CVD processes showed poor selectivity due to nucleation on the nongrowth surfaces. Since ALD is more strongly dependent on the surface properties, there is room for developing more robust selective chemistries enabling self-aligned ALD.

Two studies in which self-aligned ALD has been used to fabricate nanoscale devices are describes here to further explain this technology. A recent study by Selvaraj *et al.* explored the synthesis of copper diffusion barrier layers by selective ALD growth.[112] Essential for this application is that the diffusion barrier material is selectively deposited on the interlayer dielectric surfaces, while the growth on the adjacent copper surfaces is prevented. Moreover, the copper should not oxidize during the deposition as this leads to degraded electrical and mechanical properties. In previous work of the same group it was found that the selectivity of metal-oxide ALD (HfO_2 and TiO_2) on silicon in the presence of copper is limited to 15 - 25 cycles due to the oxidation of the copper.[58,113] Therefore, anhydrous ethanol was selected as oxidant-free reactant for ZrO_2 ALD as an alternative to water. Ethanol was shown to lead to ZrO_2 deposition, while it also reduced the copper surface during every cycle. In this way, the selective growth of ZrO_2 was prolonged to at least 70 ALD cycles. It was demonstrated that the ALD-grown ZrO_2 diffusion barriers can withstand temperatures up to 700 °C.[112]

Another example of self-aligned ALD has been reported by Farmer *et al.* in which the nucleation difficulties of ALD on graphene were exploited in the fabrication of graphene field-effect transistors (FET).[114] Figure 15 shows a schematic of the fabrication process. First, a dielectric layer and a top gate (TG) electrode are patterned on an exfoliated graphene flake. Self-aligned ALD is subsequently used to electrically isolate the gate electrode from the source and the drain electrodes. Because of the chemical inertness of graphene towards ALD, growth of Al_2O_3 only occurs on the top gate, and on the sidewalls of the top gate dielectric, and not on the graphene channel. Finally, the source and the drain electrodes are patterned, which are then electrically isolated from the top gate by the Al_2O_3 deposited in the previous step. This fabrication process allowed for reduction of the access length between the gate and the source/drain electrodes to 15 - 20 nm.[114]

The examples illustrate that self-aligned ALD growth involves selective ALD on certain materials, while keeping other surfaces in the same state. In both cases, it was crucial for device functioning to avoid the ALD growth on the critical component of the device, i.e. the copper interconnect and the graphene channel. Especially in the example of the graphene FET it is essential to use a self-aligned fabrication scheme, because lithography at this scale with a good overlay is extremely difficult.

To further explore the application possibilities of self-aligned ALD growth, selective ALD processes for various materials are needed. For self-aligned metal ALD, conditions similar to those employed in area-selective ALD by area-activation (i.e. low reactant exposure, low substrate temperature) can be used to achieve selective growth. Self-aligned metal-oxide or metal-nitride ALD is more challenging, as these ALD processes readily nucleate on most surfaces. For these materials, the best approach may be to deactivate the growth on the nongrowth surfaces by selectively adsorbing,

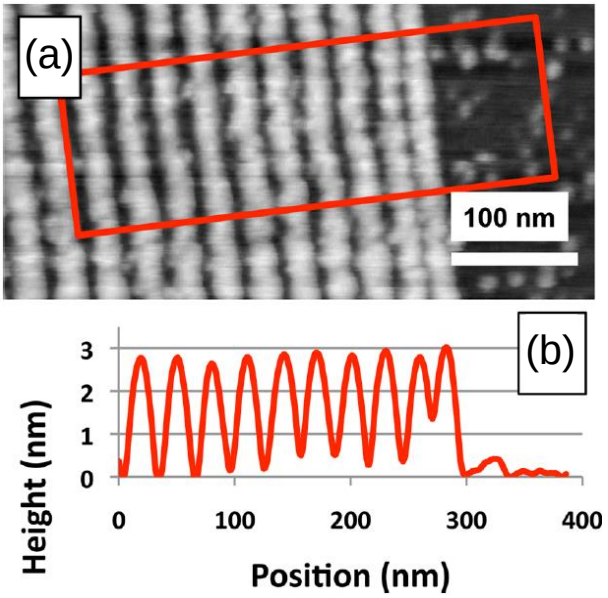

Fig. 14 (a) Atomic force microscopy (AFM) image of TiO_2 nanostructures fabricated by STM lithography and 80 ALD cycles. (b) Cross-section of the area indicated in (a) showing lines of 2.8 nm height and 15 nm width. Reprinted (adapted) with permission from (S. McDonnell *et al.*, *J. Phys. Chem. C*, 2013, **117**, 20250.). Copyright (2013) American Chemical Society.

for example, self-assembled monolayers (See Fig. 9). Since most device architectures consists of many different materials, it is often not sufficient to have selectivity between two different surfaces. ALD growth should be avoided on all the surfaces for which the presence of a film would be detrimental for device functioning. Therefore, a better understanding of the nucleation of ALD processes on various surfaces is required.

VI. Fabrication of nanostructures by exploiting selective deposition

The work on area-selective ALD inspired some novel approaches for the synthesis of specific nanostructures. In this section it is illustrated how selective ALD methods have been exploited for the synthesis of nanoparticles with size and density control, core/shell nanoparticles, oxide nanotubes, and nanowires. In addition, it is discussed how sequential infiltration synthesis (SIS, see Sec. III.B.) can be applied to block copolymers (BCPs) to fabricate nanostructures.

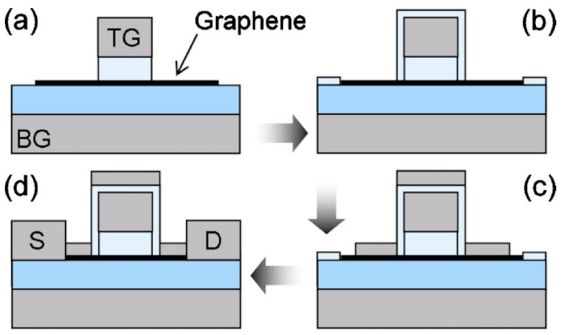

Fig. 15 Schematic representation of the fabrication scheme for graphene field-effect transistors developed by Farmer *et al.* In step (b) Al_2O_3 is selectively deposited on the top gate (TG) and the sidewalls of the top gate dielectric, while no growth takes place on the graphene channel. The fabrication of the transistor is completed with (c,d) the deposition of the source and drain electrodes using two deposition steps. Reprinted with permission from [D.B. Farmer *et al.*, *Appl. Phys. Lett.*, 2010, **97**, 013103]. Copyright [2010], AIP Publishing LLC.

A. Nanoparticles with size and density control

Metallic nanoparticles are often used in catalysis applications because of their enhanced catalytic activity and high surface-to-volume ratio.[115] Since the catalytic activity for most chemical reactions depends strongly on the particle size,[116,117] the synthesis of nanoparticles with a narrow size distribution and a high density is an important topic in catalysis.[118]

Based on their experience with area-selective ALD involving SAMs, Bent and co-workers developed a method for the deposition of Pt nanoparticles with control of nanoparticle size and areal density.[119] They exploited the fact that ALD growth can initiate at defects in SAMs, in case the SAM is prepared using short formation times (as discussed in Sec. IV.B.).[6] For Pt ALD on a SAM-covered surface, they showed that this results in small nanoparticles at the defect sites. The areal density of the defects, and thereby the density of the Pt nanoparticles, was controlled by changing the SAM dip time (See Fig. 16a). Figure 16b shows that a constant nanoparticle size was obtained as a function of the dip time for 50 cycles ALD, but with a nanoparticle density that strongly decreases with the dip time. In addition, it was demonstrated that the particle size can be controlled with the number of ALD cycles. The mean nanoparticle diameter, as well as the Pt atomic percentage, increase with the number of cycles, as plotted in Fig. 16d for a dip time of four hours. The combination of these two parameters allows for the deposition of Pt nanoparticles with control of the particle density and size.

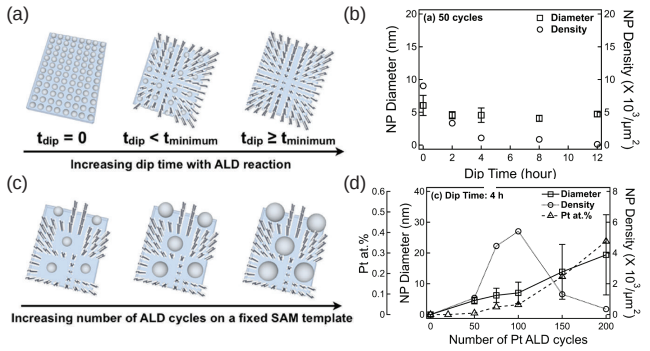

Fig. 16 Illustrations and results of the approach developed by Lee *et al*, for growing Pt nanoparticles with size and density control. (a,b) The number of defects in the SAM is tuned by changing the dip time during SAM formation, and this determines the nanoparticle density. (c,d) The particle size is controlled with the number of ALD cycles. The nanoparticle density reaches a maximum after 100 cycles and then decreases due to coalescence. Reprinted (adapted) with permission from (H-B-R Lee *et al.*, *Chem. Mater.*, **24**, 4051 (2012)). Copyright (2012) American Chemical Society.

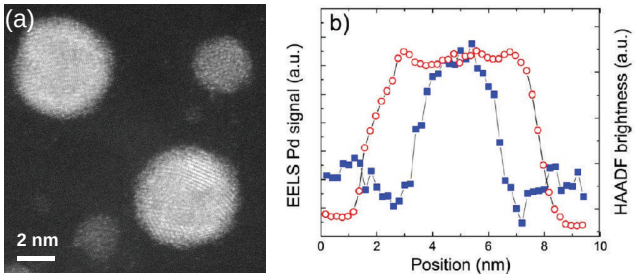

Fig. 17 (a) Transmission electron microscopy (TEM) image of Pd/Pt core/shell nanoparticles deposited by 200 cycles Pd ALD and 50 cycles Pt ALD. (b) Electron energy loss spectroscopy (EELS) line scan (square symbols) on a Pd/Pt core/shell nanoparticle. The HAADF brightness profile (circle symbols) shows the full diameter of the particle (∼5.5 nm). The difference between the two graphs reveals that Pd is only present in the core. Reprinted (adapted) with permission from (M. J. Weber *et al.*, *Chem. Mater.*, 2012, **24**, 2973). Copyright (2013) American Chemical Society.

B. Supported core/shell bimetallic nanoparticles

In addition to the control of particle size and density, within catalysis there is also interest in tuning the composition of the nanoparticles for specific chemical reactions. Bimetallic alloyed nanoparticles or core/shell nanoparticles often exhibit improved catalytic performance as compared to monometallic particles.[120,121] For example Pd/Pt core/shell nanoparticles are considered for methanol fuel cells due to their high catalytic activity for oxygen reduction and methanol electro-oxidation reactions.[122,123] Inspired by the work on area-selective ALD of Pt on seed layer patterns prepared by EBID,[7] recently an approach for synthesis of Pt/Pd and Pd/Pt core/shell nanoparticles was developed.[124] As discussed in Sec. IV.C., the nucleation behavior of thermal ALD of Pt can be tuned such that growth is selectively obtained on a seed layer pattern.[96] The same conditions were employed for the deposition of the Pt shell on Pd nanoparticles, with the aim of selectively coating the Pd shell, while preventing the formation of Pt nanoparticles on the support material.

Figure 17a shows a transmission (TEM) electron microscopy image of Pd/Pt core/shell nanoparticles synthesized by 200 cycles Pd ALD, followed by 50 cycles Pt ALD using selective growth conditions (i.e. a low O_2 pressure of 0.01 Torr). A difference between the Pd core and the Pt shell is visible in the image; the lattice fringes in the Pt shell do not continue in the Pd core. An electron energy loss spectroscopy (EELS) line scan on a core/shell nanoparticle is depicted in Fig. 17b, which reveals that Pd is only present in the ∼3.5 nm core, thereby proving the core/shell structure of the nanoparticle. The atomic level control of ALD is expected to enable the synthesis of core/shell nanoparticles with control of the core and shell dimensions.

The application of selective ALD to the synthesis of supported bimetallic nanoparticles was recently extended by Lu *et al.* to all combinations of Pd, Ru and Pt metals.[125] All the depositions were carried out at 150 °C to facilitate the synthesis of core/shell as well as alloyed nanoparticles. To this end, thermal ALD processes were investigated that nucleate at 150 °C, but also processes that lead to selective growth at 150 °C on a metal core without nucleation on the oxide support. For example, Pd ALD from $Pd(hfac)_2$ and HCHO was shown to result in growth on oxides, while Pd ALD from $Pd(hfac)_2$ and H_2 was used for selective ALD on the metal cores (Ru or Pt).[125]

C. TiO_2 and ZrO_2 nanotubes

Inspired by the research on carbon nanotubes, the synthesis of one-dimensional nanotubes of various materials has attracted attention in the last decade. The fabrication of TiO_2 nanotubes has been investigated extensively, because of the catalytic properties of this material. The structure of a nanotube is interesting for certain catalysis applications due to its high surface area. Shin *et al.* used SAMs for the deactivation of ALD growth in an approach enabling synthesis of TiO_2 and ZrO_2 nanotubes.[126] ALD was carried out on a membrane of nanoporous polycarbonate (PC) used as template. To eliminate post-deposition processing by etching, ALD was performed selectively in the pores of the PC membrane, while the growth on the top and bottom side of the PC membrane was blocked by ODTS SAMs patterned by microcontact printing. The PC material was dissolved afterwards in chloroform, re-

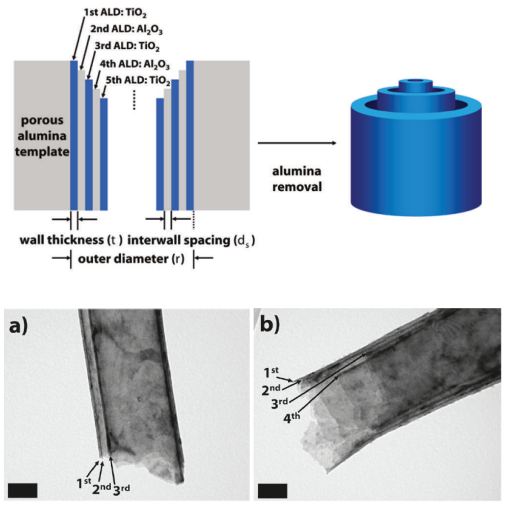

Fig. 18 Schematic representation of the approach for synthesis of anatase TiO_2 multi-walled nanotubes as reported by Bae *et al.*[127] A multilayer stack of Al_2O_3 and TiO_2 was deposited on a nanoporous polycarbonate (PC) template. Subsequently, the template and the Al_2O_3 were etched away, resulting in multi-walled TiO_2 nanotubes. In addition, SEM images of (a) triple- and (b) quadruple-walled nanotubes are shown. Reprinted (adapted) with permission from (C. Bae *et al.*, *Chem. Mater.*, 2009, **21**, 2574). Copyright (2009) American Chemical Society.

sulting in separate metal-oxide nanotubes.

In an extension of this approach, multi-walled anatase TiO_2 nanotubes were fabricated as shown in Fig. 18.[127] These multi-walled tubes were synthesized by alternating between the ALD processes of TiO_2 and Al_2O_3, followed by selective etching of the Al_2O_3 and the template material.

D. Pt nanowires on ordered pyroloytic graphite

A new method for synthesis of Pt nanowires on highly ordered pyrolytic graphite (HOPG) has recently been developed by Lee *et al.*[128] As a motivation of the study, it was mentioned that Pt nanoparticles on a carbon support migrate, coalesce, and become detached, which has a negative effect of the catalytic performance of the catalyst. Pt nanowires can also be used for specific catalysis applications, while they show a better structural stability than Pt nanoparticles, limiting the degradation of the catalyst.

HOPG consists of stacked graphene layers on which it is difficult to obtain Pt ALD growth. However, Pt ALD was shown to initiate on the step edges of the HOPG, where defects are present, which results in laterally aligned nanowires. Initially, Pt nanoparticles are formed at these defects, but the Pt nanoparticles coalesce at some point during the deposition resulting in a Pt nanowire. No nucleation on the chemically

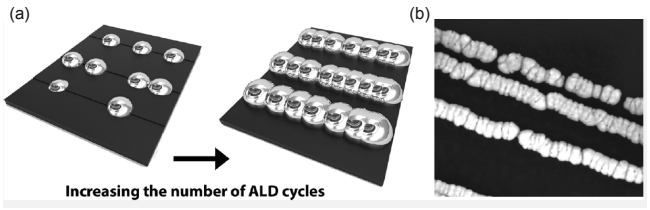

Fig. 19 (a) Schematic representation of the synthesis of Pt nanowires by ALD on highly ordered pyrolytic graphite. Pt nanoparticles are formed at the step edges, and coalesce during the deposition resulting in a Pt nanowire. (b) Scanning electron microscopy (SEM) image of a Pt nanowire synthesized using this approach. Reprinted (adapted) with permission from (H-B-R Lee *et al.*, *Nano Lett.*, 2013, **13**, 457.). Copyright (2013) American Chemical Society.

inert basal planes of the HOPG was observed, indicating that the growth occurs selectively at the step edges. It was demonstrated in the study that the height and width of the nanowires can be controlled by the number of ALD cycles.

E. Sequential infiltration synthesis in block copolymers

As already briefly discussed in Sec. III.B., block copolymers (BCP) can self-assemble into morphologies with tunable shape and size, which gives unique possibilities for the synthesis of nanostructured materials. For certain ALD processes, it is possible to selectively deposit in one of the domains of the BCP. This has been applied in BCP lithography (see Sec. III.B.), but also for the synthesis of various nanostructures, as is discussed in more detail here. This work has been inspired by early reports in which ALD was used to deposit on the boundary surface of BCP templates.[129,130] However, here we focus on studies exploiting selective growth in one of the BCP domains to fabricate specific nanostructures. There is recently also much interest for the synthesis of mesoporous metal-oxide networks[131–133], or nanotube arrays[134,135] by using BCPs as a template for ALD (without selectivity of the ALD growth), but this beyond the scope of this review.

Peng *et al* demonstrated that SIS can be used to modify the properties and dimensions of periodic nanostructures synthesized using BCPs.[136] SIS of Al_2O_3 and TiO_2 was carried out on polystyrene-*block*-poly(methyl methacrylate) (PS-*b*-PMMA).[136] During SIS, the metal precursors $TiCl_4$, $AlCl_3$, or $Al(CH_3)_3$ selectively react with the carbonyl groups in the PMMA microdomains, while no growth takes place in the polystyrene regions due to the inert chemistry of polystyrene. The adsorbed metal precursors act as nucleation sites for subsequent SIS growth. The dimensions of the structures are determined by the number of reactive sites in a domain and the number of SIS cycles that are carried out. This gives the opportunity to tune the dimensions of the inorganic domains be-

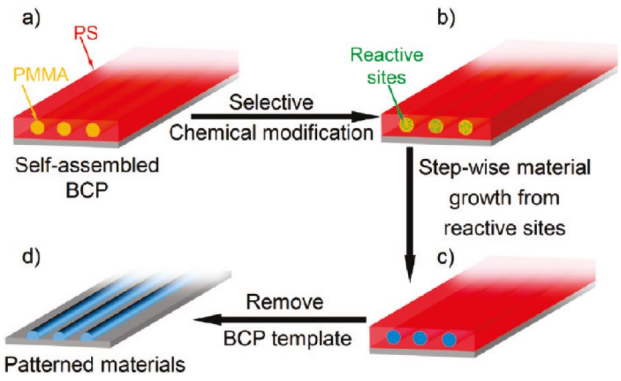

Fig. 20 Schematic representation of the modification of block copolymers using the sequential infiltration synthesis (SIS) technique.[137] (a) First one cycle of Al_2O_3 SIS is performed to selectively generate active surface sites in the PMMA blocks on which different SIS processes can initiate. (b) The amount of deposited material and thereby the dimensions of the final structures can be tuned by performing a certain number of SIS cycles. (c) After SIS, the block copolymer template is removed by an anneal or a plasma treatment. Reprinted (adapted) with permission from (Q.Peng *et al.*, *ACS Nano*, 2011, **5**, 4600). Copyright (2011) American Chemical Society.

yond the dimensions of the initial PMMA domains offering additional flexibility. The procedure is completed with a thermal anneal or plasma treatment in which the polymer template is removed leaving behind the patterned inorganic material. In a follow-up paper, it was shown that a variety of materials can be deposited in the PMMA domains of PS-*b*-PMMA by first performing 1 SIS cycle of Al_2O_3, and then switching to the SIS process of for example SiO_2, ZnO or W (See Fig. 20).[137] The -Al-CH_3/-Al-OH groups formed during the Al_2O_3 SIS cycle provide reactive surface sites where the growth of these other materials can initiate.

In recent work, the approach developed by Peng *et al.* has been used to deposit various nanostructures, such as nanopatterned arrays of ZnO stuctures,[138] and hexagonally packed TiO_2 nanoparticles.[139] Kamcev *et al.* improved the block-selective affinity of ALD precursors by including an ultraviolet (UV) light treatment before SIS in PS-*b*-PMMA BCPs.[140] It was shown that the UV treatment results in the formation of oxygen-containing functional groups within the polystyrene regions. This allows for SIS in the polystyrene domains, which is in contrast to the conventional approach that leads to growth in the PMMA domains.

VII. Conclusions

The role of ALD in advanced lithographic schemes is gaining traction, because of the ability of ALD to deposit conformal films at low substrate temperatures, and because it can infiltrate in porous materials. In direct spacer defined double patterning (D-SDDP), the use of ALD allows for the elimination of several processing steps since it enables the deposition of a conformal layer of inorganic material directly on a polymer resist pattern. Another form of ALD-enabled nanopatterning is the use of ALD to modify the properties of resist films. In block copolymer lithography, ALD has been applied to selectively deposit in one of the polymer blocks in order to make it more resistant to plasma etching.

Most applications using ALD-grown films require the patterning of the film. In addition to the conventional patterning approach based on etching, several approaches for film structuring were described in this review, i.e. patterning based on lithography and lift-off, area-selective ALD by area-deactivation, and area-selective ALD by area-activation. Table 5 presents an overview of the characteristics of these different patterning approaches. Area-selective ALD approaches are generally less complex than conventional lithography-based approaches (i.e. involve fewer processing steps). On the other hand, lithography, etching, and lift-off, are well-established processing techniques that have been applied extensively in the microelectronics industry. The selection of one of these approaches for a certain application, depends mostly on the compatibility of the different processing steps involved with the elements of the existing device structure. Lift-off methods are used when etching needs to be avoided on sensitive device structures. For area-selective ALD by area-deactivation, only growth is obtained in those regions where it is desired, which eliminates the need for complicated lift-off steps. And finally, area-selective ALD by area-activation is completely free of etching and lift-off steps, and even eliminates the use of sticky resist films, but is currently limited to only a few ALD processes.

Motivated by the ongoing miniaturization in microelectronics, it can be expected that selective ALD will keep on gaining attention. Especially when extremely small nanoscale features need to be synthesized, it can be beneficial to process the material in a bottom-up fashion using self-aligned growth to avoid overlay challenges. The strong dependence of ALD on surface chemistry, gives unique opportunities to develop robust selective growth processes.

Acknowledgments

The authors would like to thank dr. S.E. Potts, S.A.F. Dielissen, and N.F.W. Thissen for fruitful discussions. This work is supported by NanoNextNL, a micro- and nanotechnology programme of the Dutch ministry of economic affairs, agriculture and innovation (EL&I) and 130 partners. The research of W.M.M.K. and A.A.B. has been made possible by the Netherlands Organization for Scientific Research (NWO, VICI and

Table 5 Overview of the approaches for the patterning of ALD films described in this review. The temperature refers to the substrate temperature during ALD.

Approach	Complexity: # of steps	Low temp. required?	Etching required?	Lift-off required?	Polymer film / SAM involved?
Patterning based on lithography and etching	≥ 6	No	Yes	No	Yes
Patterning based on lithography and lift-off	≥ 5	Yes	No	Yes	Yes
Area-selective ALD by area-deactivation	≥ 3	Yes	No	No	Yes
Area-selective ALD by area-activation	2	No	No	No	No

VIDI programs respectively).

References

1 M. Leskelä and M. Ritala, *Thin Solid Films*, 2002, **409**, 138.
2 S. M. George, *Chem. Rev.*, 2010, **110**, 111.
3 M. J. Biercuk, D. J. Monsma, C. M. Marcus, J. S. Becker and R. G. Gordon, *Appl. Phys. Lett.*, 2003, **83**, 2405.
4 H.-B.-R. Lee and S. F. Bent, *Nanopatterning by Area-Selective Atomic Layer Deposition*, in, "Atomic layer deposition of nanostructured materials, N. Pinna, and M. Knez, Wiley, 2012.
5 M. Knez, K. Nielsch and L. Niinistö, *Adv. Mater.*, 2007, **19**, 3425.
6 X. Jiang and S. F. Bent, *J. Phys. Chem. C*, 2009, **113**, 17613.
7 A. J. M. Mackus, J. J. L. Mulders, M. C. M. van de Sanden and W. M. M. Kessels, *J. Appl. Phys.*, 2010, **107**, 116102.
8 E. Färm, S. Lindroos, M. Ritala and M. Leskelä, *Chem. Mater.*, 2012, **24**, 275.
9 J. Beynet, P. Wong, A. Miller, S. Locorotondo, D. Vangoidsenhoven, T.-H. Yoon, M. Demand, H.-S. Park, T. Vandeweyer, H. Sprey, Y.-M. Yoo and M. Maenhoudt, *Proc. SPIE*, 2009, **7520**, 75201J.
10 H. B. Profijt, S. E. Potts, M. C. M. van de Sanden and W. M. M. Kessels, *J. Vac. Sci. Technol. A*, 2011, **29**, 050801.
11 I. J. Raaijmakers, *ECS Trans.*, 2011, **41**, 3.
12 D. Shamiryan, V. Paraschiv, W. Boullart and M. R. Baklanov, *High Energ. Chem.*, 2009, **43**, 204.
13 J. W. Coburn and H. F. Winters, *J. Appl. Phys.*, 1979, **50**, 3189.
14 M. Geissler and Y. Xia, *Adv. Mater.*, 2004, **16**, 1249.
15 A. E. Grigorescu and C. W. Hagen, *Nanotechnology*, 2009, **20**, 292001.
16 A. Pimpin and W. Srituravanich, *Engineering Journal*, 2012, **16**, 37.
17 X. Jiang, R. Chen and S. F. Bent, *Surf. Coat. Technol.*, 2007, **201**, 8799.
18 J. A. DeFranco, B. S. Schmidt, M. Lipson and G. G. Malliaras, *Org. Electron.*, 2006, **7**, 22.
19 M. E. Bahlke, H. A. Mendoza, D. T. Ashall, A. S. Yin and M. A. Baldo, *Adv. Mater.*, 2012, **24**, 6136.
20 K. R. Williams, K. Gupta and M. Wasilik, *J. Microelectromech. Syst.*, 2003, **12**, 761.
21 S. Owa and H. Nagasaka, *Proc. SPIE*, 2008, **7140**, 714015.
22 Y. Borodovsky, *Proc. SPIE*, 2006, **6153**, 615301.
23 R. P. Seisyan, *Technical Physics*, 2011, **56**, 1061.
24 S. Lee, J. Byers, K. Jen, P. Zimmerman, B. Rice, N. J. Turro and C. G. Willson, *Proc. SPIE*, 2008, **6924**, 69242A.
25 J. Versluijs, Y. Kong Siew, E. Kunnen, D. Vangoidsenhoven, S. Demuynck, V. Wiaux, H. Dekkers and G. Beyer, *Proc. SPIE*, 2011, **7973**, 79731R.
26 A. Niroomand, B. Zhou, R. Alapati, U.S. Patent 7,732,343 B2 (June 8, 2010).
27 J. Beynet, H. S. Park, N. Inoue, U.S. Patent 8,252,691 B2 (August 28, 2012).
28 J. W. Lim, S. J. Yun and J. H. Lee, *ETRI J.*, 2005, **27**, 118.
29 T. Murata, Y. Miyagawa, Y. Nishida, Y. Yamamoto, T. Yamashita, M. Matsuura, K. Asai and H. Miyatake, *Jpn. J. Appl. Phys.*, 2010, **49**, 04DB11.
30 H. Yaegashi, K. Oyama, K. Yabe, S. Yamauchi, A. Hara and S. Natori, *Proc. of SPIE*, 2011, **7972**, 79720B–1.
31 H. Yaegashi, K. Oyama, A. Hara, S. Natori and S. Yamauchi, *Proc. of SPIE*, 2012, **8325**, 83250B.
32 T. Oka, A. Shimizu, U.S. Patent 8,197,915 B2 (June 12, 2012).
33 J. Ha, H. Fukuda, S. Kaido, U.S. Patent application 2012/0164846 A1 (June 28, 2012).
34 S. Dhuey, C. Peroz, D. Olynick, G. Calafiore and S. Cabrini, *Nanotechnology*, 2013, **24**, 105303.
35 C. Peroz, S. Dhuey, M. Cornet, M. Vogler, D. Olynick and S. Cabrini, *Nanotechnology*, 2012, **23**, 015305.
36 Y.-C. Tseng, A. U. Mane, J. W. Elam and S. B. Darling, *Adv. Mater.*, 2012, **24**, 2608.
37 A. Sinha, D. W. Hess and C. L. Henderson, *Electrochem. Solid-State Lett.*, 2006, **9**, G330.
38 Y.-C. Tseng, Q. Peng, L. E. Ocola, D. A. Czaplewski, J. W. Elam and S. B. Darling, *J. Vac. Sci. Technol. B*, 2011, **29**, 06FG01–1.
39 M. Ramanathan, Y.-C. Tseng, K. Ariga and S. B. Darling, *J. Mater. Chem. C*, 2013, **1**, 2080.
40 S. B. Darling, J. Elam, Y. -Ch. Tseng, Q. Peng, U.S. Patent application 2012/0241411 A1 (September 27, 2012).
41 Y.-C. Tseng, Q. Peng, L. E. Ocola, J. W. Elam and S. B. Darling, *J. Phys. Chem. C*, 2011, **115**, 17725.
42 S. B. Darling, *Prog. Polym. Sci.*, 2007, **32**, 1152.
43 G. Gay, T. Baron, C. Agraffeil, B. Salhi, T. Chevolleau, G. Cunge, H. Grampeix, J.-H. Tortai, F. Martin, E. Jalaguier and B. De Salvo, *Nanotechnology*, 2010, **21**, 435301.
44 M. Ramanathan and S. B. Darling, *Polym. Int.*, 2013, **62**, 1123.
45 R. Ruiz, L. Wan, J. Lille, K. C. Patel, E. Dobisz, D. E. Johnston, K. Kisslinger and C. T. Black, *J. Vac. Sci. Technol. B*, 2012, **30**, 06F202–1.
46 R. Ruiz, E. Dobisz and T. R. Albrecht, *ACS Nano*, 2011, **5**, 79.
47 E. Färm, M. Kemell, M. Ritala and M. Leskelä, *J. Phys. Chem. C*, 2008, **112**, 15791.
48 E. Färm, M. Kemell, E. Santala, M. Ritala and M. Leskelä, *J. Electrochem. Soc.*, 2010, **157**, K10.
49 A. Sinha, D. W. Hess and C. L. Henderson, *J. Electrochem. Soc.*, 2006, **153**, G465.
50 V. Suresh, M. S. Huang, M. P. Srinivasan, C. Guan, H. J. Fan and S. Krishnamoorthy, *J. Phys. Chem. C*, 2012, **116**, 23729.
51 D. H. Levy, S. F. Nelson and D. Freeman, *J. Display Technol.*, 2009, **5**, 484.
52 M. Coll, J. Gazquez, A. Palau, M. Varela, X. Obradors and T. Puig, *Chem. Mater*, 2012, **24**, 3732.
53 J.-M. Kim, H.-B.-R. Lee, C. Lansalot, C. Dussarrat, J. Gatineau and H. Kim, *Jpn. J. Appl. Phys.*, 2010, **49**, 05FA10–1.
54 A. Sinha, D. W. Hess and C. L. Henderson, *J. Vac. Sci. Technol. B*, 2006,

24, 2523.
55 A. Sinha, D. W. Hess and C. L. Henderson, *J. Vac. Sci. Technol. B*, 2007, **25**, 1721.
56 M. M. Frank, Y. J. Chabal, M. L. Green, A. Delabie, B. Brijs, G. D. Wilk, M.-Y. Ho, E. B. O. da Rosa, I. J. R. Baumvol and F. C. Stedile, *Appl. Phys. Lett.*, 2003, **83**, 740.
57 R. L. Puurunen, W. Vandervorst, W. F. A. Besling, O. Richard, H. Bender, T. Conard, C. Zhao, A. Delabie, M. Caymax, S. De Gendt, M. Heyns, M. M. Viitanen, M. de Ridder, H. H. Brongersma, Y. Tamminga, T. Dao, T. de Win, M. Verheijen, M. Kaiser and M. Tuominen, *J. Appl. Phys.*, 2004, **96**, 4878.
58 Q. Tao, G. Jursich and C. Takoudis, *Appl. Phys. Lett.*, 2010, **96**, 192105.
59 J. Kwon, M. Saly, M. D. Halls, R. K. Kanjolia and Y. J. Chabal, *Chem. Mater.*, 2012, **24**, 1025.
60 R. Chen, H. Kim, P. C. McIntyre, D. W. Porter and S. F. Bent, *Appl. Phys. Lett.*, 2005, **86**, 191910.
61 E. K. Seo, J. W. Lee, H. M. Sung-Suh and M. M. Sung, *Chem. Mater.*, 2004, **16**, 1878.
62 J. Huang, M. Lee and J. Kim, *J. Vac. Sci. Technol. A*, 2012, **30**, 01A128.
63 M. H. Park, Y. J. Jang, H. M. Sung-suh and M. M. Sung, *Langmuir*, 2004, **20**, 2257.
64 E. Färm, M. Kemell, M. Ritala and M. Leskelä, *Thin Solid Films*, 2008, **517**, 972.
65 M. Yan, Y. Koide, J. R. Babcock, P. R. Markworth, J. A. Belot, T. J. Marks and R. P. H. Chang, *Appl. Phys. Lett.*, 2001, **79**, 1709.
66 F. S. M. Hashemi, C. Prasittichai and S. F. Bent, *J. Phys. Chem. C*, 2014, **118**, 10957.
67 W. Lee and F. B. Prinz, *J. Electrochem. Soc.*, 2009, **156**, G125.
68 J. P. Lee and M. M. Sung, *J. Am. Chem. Soc.*, 2004, **126**, 28.
69 J. Liu, Y. Mao, E. Lan, D. Rey Banatao, G. J. Forse, J. Lu, H.-O. Blom, T. O. Yeates, B. Dunn and J. P. Chang, *J. Am. Chem. Soc.*, 2008, **130**, 16908.
70 R. Chen and S. F. Bent, *Adv. Mater.*, 2006, **18**, 1086.
71 W. Lee, N. P. Dasgupta, O. Trejo, J.-R. Lee, J. Hwang, T. Usui and F. B. Prinz, *Langmuir*, 2010, **26**, 6845.
72 H.-B.-R. Lee, W.-H. Kim, J. W. Lee, J.-M. Kim, K. Heo, I. C. Hwang, Y. Park, S. Hong and H. Kim, *J. Electrochem. Soc.*, 2010, **157**, D10.
73 W.-H. Kim, H.-B.-R. Lee, K. Heo, Y. K. Lee, T.-M. Chung, C. G. Kim, S. Hong, J. Heo and H. Kim, *J. Electrochem. Soc.*, 2011, **158**, D1.
74 K. J. Park, J. M. Doub, T. Gougousi and G. N. Parsons, *Appl. Phys. Lett.*, 2005, **86**, 051903.
75 E. Färm, M. Kemell, M. Ritala and M. Leskelä, *Chem. Vap. Deposition*, 2006, **12**, 415.
76 E. Färm, M. Vehkamäki, M. Ritala and M. Leskelä, *Semicond. Sci. Technol.*, 2012, **27**, 074004.
77 X. Jiang and S. F. Bent, *J. Electrochem. Soc.*, 2007, **154**, D648.
78 C. Prasittichai, H. Zhou and S. F. Bent, *ACS Appl. Mater. Interfaces*, 2013, **5**, 13391.
79 H.-B.-R. Lee, J. Kim, H. Kim, W.-H. Kim, J. W. Lee, and I. Hwang, *J. Korean Phys. Soc.*, 2010, **56**, 104.
80 R. Chen, H. Kim, P. C. McIntyre and S. F. Bent, *Appl. Phys. Lett.*, 2004, **84**, 4017.
81 R. Chen, H. Kim, P. C. Mcintyre and S. F. Bent, *Chem. Mater.*, 2005, **17**, 536.
82 R. Chen and S. F. Bent, *Chem. Mater.*, 2006, **18**, 3733.
83 J. P. Lee, Y. J. Jang and M. M. Sung, *Adv. Funct. Mater.*, 2003, **13**, 873.
84 M. Li, M. Dai and Y. J. Chabal, *Langmuir*, 2009, **25**, 1911.
85 O. Seitz, M. Dai, F. S. Aguirre-Tostado, R. M. Wallace and Y. J. Chabal, *J. Am. Chem. Soc.*, 2009, **131**, 18159.
86 D. H. Levy, C. R. Ellinger and S. F. Nelson, *Appl. Phys. Lett.*, 2013, **103**, 043505.
87 D. H. Levy and S. F. Nelson, *J. Vac. Sci. Technol. A*, 2012, **30**, 018501.
88 Y. Hua, W. P. King and C. L. Henderson, *Microelectron. Eng.*, 2008, **85**, 934.
89 M. Coll, A. Palau, J. Gonzalez-Rosillo, J. Gazquez, X. Obradors and T. Puig, *Thin Solid Films*, 2014, **553**, 7.
90 K. J. Park and G. N. Parsons, *Appl. Phys. Lett.*, 2006, **89**, 043111.
91 M. N. Mullings, H.-B.-R. Lee, N. Marchack, X. Jiang, Z. Chen, Y. Gorlin, K.-P. Lin and S. F. Bent, *J. Electrochem. Soc.*, 2010, **157**, D600.
92 R. H. A. Ras, E. Sahramo, J. Malm, J. Raula and M. Karppinen, *J. Am. Chem. Soc.*, 2008, **130**, 11252.
93 A. J. M. Mackus, N. F. W. Thissen, J. J. L. Mulders, P. H. F. Trompenaars, M. A. Verheijen, A. A. Bol and W. M. M. Kessels, *J. Phys. Chem. C*, 2013, **117**, 10788.
94 H. C. M. Knoops, A. J. M. Mackus, M. E. Donders, M. C. M. van de Sanden, P. H. L. Notten and W. M. M. Kessels, *Electrochem. Solid-State Lett.*, 2009, **12**, G34.
95 A. J. M. Mackus, N. Leick, L. Baker and W. M. M. Kessels, *Chem. Mater.*, 2012, **24**, 1752.
96 A. J. M. Mackus, M. A. Verheijen, N. Leick, A. A. Bol and W. M. M. Kessels, *Chem. Mater.*, 2013, **25**, 1905.
97 A.F. de Jong, J.J.L. Mulders, W.M.M. Kessels, and A.J.M. Mackus, U.S. Patent No. 8,268,532 B2 (September 18, 2012).
98 A. J. M. Mackus, S. A. F. Dielissen, J. J. L. Mulders and W. M. M. Kessels, *Nanoscale*, 2012, **4**, 4477.
99 A. Botman, J. J. L. Mulders, R. Weemaes and S. Mentink, *Nanotechnology*, 2006, **17**, 3779.
100 J. M. De Teresa, R. Córdoba, A. Fernández-Pacheco, O. Montero, P. Strichovanec and M. R. Ibarra, *J. Nanomater.*, 2009, **2009**, 936863.
101 M. Weber, H. W. P. Koops, M. Rudolph, J. Kretz and G. Schmidt, *J. Vac. Sci. Technol. B*, 1995, **13**, 1364.
102 P. Martensson and J.-O. Carlsson, *J. Electrochem. Soc.*, 1998, **145**, 5.
103 R. Gupta and B. G. Willis, *Appl. Phys. Lett.*, 2007, **90**, 253102.
104 S. McDonnell, R. C. Longo, O. Seitz, J. B. Ballard, G. Mordi, D. Dick, J. H. G. Owen, J. N. Randall, J. Kim, Y. J. Chabal, K. Cho and R. M. Wallace, *J. Phys. Chem. C*, 2013, **117**, 20250.
105 T. Aaltonen, A. Rahtu, M. Ritala and M. Leskelä, *Electrochem. Solid-State Lett.*, 2003, **6**, C130.
106 N. Leick, S. Agarwal, A. J. M. Mackus, S. E. Potts and W. M. M. Kessels, *J. Phys. Chem. C*, 2013, **117**, 21320.
107 T. Aaltonen, P. Alén, M. Ritala and M. Leskelä, *Chemical Vap. Deposition*, 2003, **9**, 45.
108 R. C. Longo, S. McDonnell, D. Dick, R. M. Wallace, Y. J. Chabal, J. H. G. Owen, J. B. Ballard, J. N. Randall and K. Cho, *J. Vac. Sci. Technol. B*, 2014, **32**, 03D112.
109 A. Pirkle, J. Chan, A. Venugopal, D. Hinojos, C. W. Magnuson, S. McDonnell, L. Colombo, E. M. Vogel, R. S. Ruoff and R. M. Wallace, *Appl. Phys. Lett.*, 2011, **99**, 122108.
110 Y.-C. Lin, C.-C. Lu, C.-H. Yeh, C. Jin, K. Suenaga and P.-W. Chiu, *Nano Lett.*, 2012, **12**, 414.
111 W. L. Gladfelter, *Chem. Mater.*, 1993, **5**, 1372.
112 S. K. Selvaraj, J. Parulekar and C. G. Takoudis, *J. Vac. Sci. Technol. A*, 2014, **32**, 010601.
113 Q. Tao, K. Overhage, G. Jursich and C. Takoudis, *Thin Solid Films*, 2012, **520**, 6752.
114 D. B. Farmer, Y.-M. Lin and P. Avouris, *Appl. Phys. Lett.*, 2010, **97**, 013103.
115 G. A. Somorjai, H. Frei and J. Y. Park, *J. Am. Chem. Soc.*, 2009, **131**, 16589.
116 A. T. Bell, *Science*, 2003, **299**, 1688.
117 F. Zaera, *Catal. Lett.*, 2012, **142**, 501.
118 J. Lu and P. C. Stair, *Angew. Chem.*, 2010, **49**, 2547.
119 H.-B.-R. Lee, M. N. Mullings, X. Jiang, B. M. Clemens and S. F. Bent, *Chem. Mater.*, 2012, **24**, 4051.

120 C. J. Serpell, J. Cookson, D. Ozkaya, P. D. Beer, *Nature Chem.* **3**, 478 (2011).
121 S. Alayoglu, A. U. Nilekar, M. Mavrikakis, B. Eichhorn, *Nature Mater.* **7**, 333 (2008).
122 X. Zhao, M. Yin, L. Ma, L. Liang, C. Liu, J. Liao, T. Lu, W. Xing, *Energy Environ. Sci.* **4**, 2736 (2011).
123 A. U. Nilekar, Y. Xu, J. Zhang, M. B. Vukmirovic, K. Sasaki, R. R. Adzic, M. Mavrikakis, *Top. Catal.* **46** (2007).
124 M. J. Weber, A. J. M. Mackus, M. A. Verheijen, C. van der Marel and W. M. M. Kessels, *Chem. Mater*, 2012, **24**, 2973.
125 J. Lu, K.-B. Low, Y. Lei, J. A. Libera, A. Nicholls, P. C. Stair and J. W. Elam, *Nat. Commun.*, 2014, **5**, 3264.
126 H. Shin, D.-K. Jeong, J. Lee, M. M. Sung and J. Kim, *Adv. Mater.*, 2004, **16**, 1197.
127 C. Bae, Y. Yoon, H. Yoo, D. Han, J. Cho, B. H. Lee, M. M. Sung, M. Lee, J. Kim and H. Shin, *Chem. Mater.*, 2009, **21**, 2574.
128 H.-B.-R Lee, S. H. Baeck, T. F. Jaramillo, S. F. Bent, *Nano Lett.* **13**, 457 (2013).
129 R. H. A. Ras, M. Kemell, J. de Wit, M. Ritala, G. ten Brinke, M. Leskelä and O. Ikkala, *Adv. Mater.*, 2007, **19**, 102.
130 Y. Wang, Y. Qin, A. Berger, E. Yau, C. C. He, L. B. Zhang, U. Gosele and M. Knez, M. amd Steinhart, *Adv. Mater.*, 2009, **21**, 2763.
131 A. Andreozzi, L. Lamagna, G. Seguini, M. Fanciulli, S. Schamm-Chardon, C. Castro and M. Perego, *Nanotechnology*, 2011, **22**, 335303.
132 F. Li, X. Yao, Z. Wang, W. Xing, W. Jin, J. Huang and Y. Wang, *Nano Lett.*, 2012, **12**, 5033.
133 E. Kim, Y. Vaynzof, A. Sepe, S. Guldin, M. Scherer, P. Cunha, S. V. Roth and U. Steiner, *Adv. Funct. Mater.*, 2014, **24**, 863.
134 J. Yin, X. Yao, J.-Y. Liou, W. Sun, Y.-S. Sun and Y. Wang, *ACS Nano*, 2013, **7**, 9961.
135 S. J. Ku, G. C. Jo, C. H. Bak, S. M. Kim, Y. R. Shin, K. H. Kim, S. H. Kwon and J.-B. Kim, *Nanotechnology*, 2013, **24**, 085301.
136 Q. Peng, Y.-C. Tseng, S. B. Darling and J. W. Elam, *Adv. Mater.*, 2010, **22**, 5129.
137 Q. Peng, Y.-C. Tseng, S. B. Darling and J. W. Elam, *ACS Nano*, 2011, **5**, 4600.
138 V. Suresh, M. S. Huang, M. P. Srinivasan and S. Krishnamoorthy, *ACS Appl. Mater. Interfaces*, 2013, **5**, 5727.
139 J. Yin, Q. Xu, Z. Wang, X. Yao and Y. Wang, *J. Mater. Chem. C*, 2013, **1**, 1029.
140 J. Kamcev, D. S. Germack, D. Nykypanchuk, R. B. Grubbs, C.-Y. Nam and C. T. Black, *ACS Nano*, 2013, **7**, 339.